SLAC-PUB-2796
CALT-68-853
September 1981
(T/E)

RECENT RESULTS FROM THE CRYSTAL BALL*

Frank C. Porter
(Representing the Crystal Ball Collaboration)[1]
Physics Department
California Institute of Technology
Pasadena, California 91125

and

Stanford Linear Accelerator Center
Stanford University, Stanford, California 94305

(Presented at the SLAC Summer Institute on Particle Physics,
Stanford, California, July 27-August 7, 1981.)

---

* Work supported in part by the Department of Energy under contracts DE-AC03-81ER40050 (CIT) and DE-AC03-76SF00515 (SLAC).

I. INTRODUCTION

During the past year, the Crystal Ball experiment has continued the investigation of e^+e^- interactions at SPEAR. In the course of the year, we have slightly more than doubled the available datasets at the J/ψ (to 2.2×10^6 produced J/ψ) and the ψ' (to 1.8×10^6 produced ψ') resonances, and have increased the data in the 5.2 to 7.4 GeV center-of-mass ($E_{c.m.}$) region. I will limit the present discussion to recent results obtained with the J/ψ and ψ' datasets, primarily dealing with transitions among the charmonium bound states. For other recent work not covered here, I refer the interested reader to earlier talks, including: the measurement of the two photon processes[2] $\gamma\gamma \to f^o \to \pi^o\pi^o$ and $\gamma\gamma \to A_2 \to \eta\pi^o$; a search for the decay $J/\psi \to \gamma$ + axion;[3] and a new measurement of $R(e^+e^- \to \text{hadrons})$ in the 5 to 7 GeV center-of-mass energy region.[4]

To set the stage, let us briefly review the current situation in the study of the $c\bar{c}$ bound state system. Figure 1 shows the expected spectrum[5] of charmonium bound states, according to the usual non-relativistic potential-model picture. Also shown are some of the predicted radiative transitions between levels. All of the transitions (electric dipole) between the $^3S_1$ (J/ψ and ψ') states and the ^3P_J ($\chi_{0,1,2,}$) states have been observed, but the rates have large errors. The rates for[6] $\psi' \to \gamma\chi$ appear to be substantially smaller than the potential model predictions (e.g., Refs. 7 and 8), so it is important to measure these rates well, also to obtain the relative rates, for which there is less uncertainty in the theoretical predictions. In addition, there exists a strong candidate for the hyperfine-split partner to the

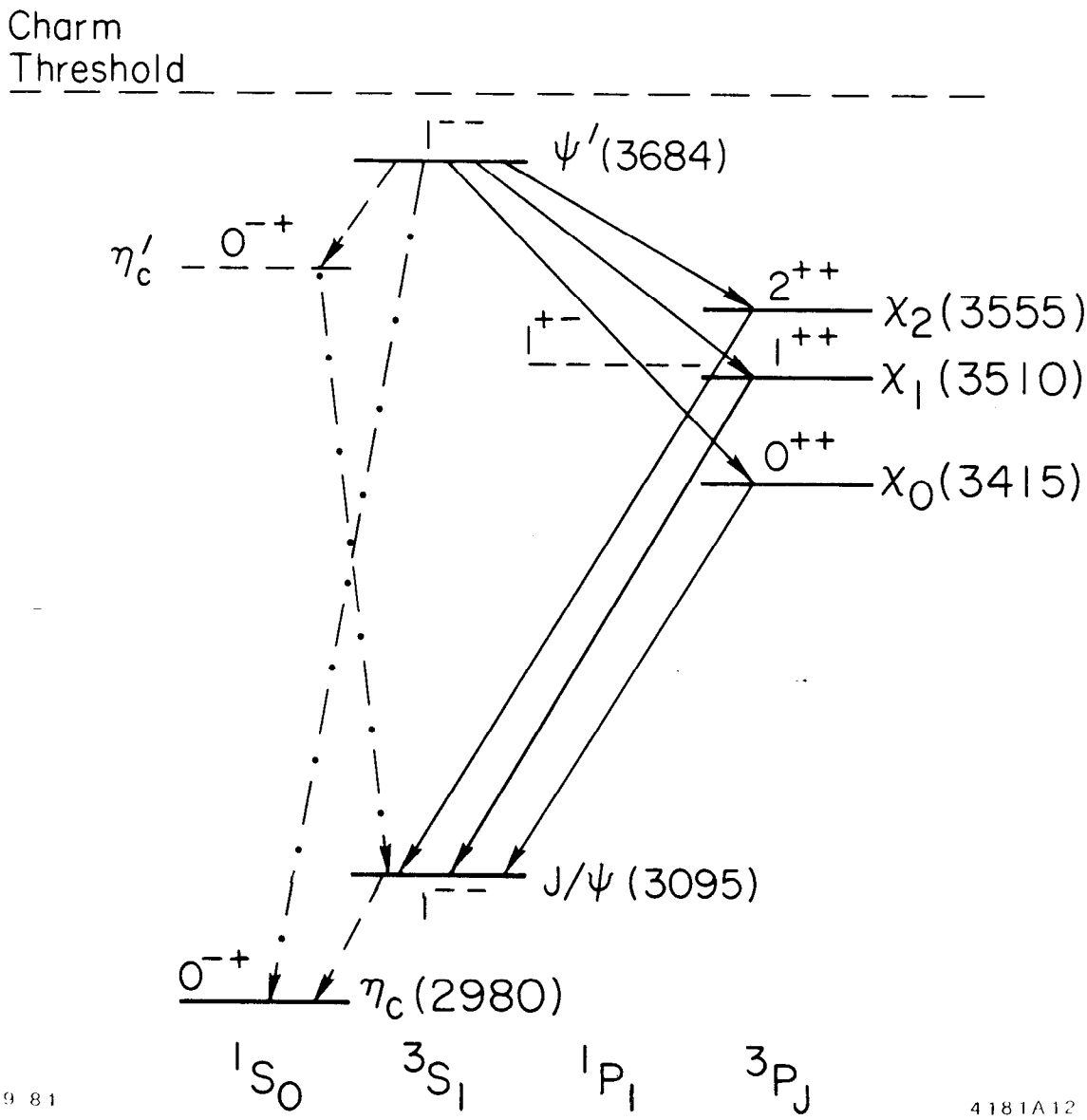

Fig. 1. The level scheme for bound state charmonium (scale approximate only). States which have not yet been observed are shown as dashed levels. The J^{PC} quantum numbers are indicated on the levels, and the spectroscopic notation $^{(2S+1)}L_J$ is shown at the bottom for each vertical grouping. Note that for $c\bar{c}$ bound states, $C = (-1)^{L+S}$, $P = -(-1)^{L}$. The arrows between states show some (but not all!) of the radiative transitions which should exist: E1 - solid arrows, allowed M1 - dashed arrows, and hindered M1 - dot-dashed arrows. The transitions involving the η' have not been previously observed. All radiative transitions which have previously been observed are shown on this figure.

J/ψ, the η_c, at a mass of about 2980 MeV.[9,10] I will, in this report, refer to this state as the η_c, although not all of its quantum numbers (e.g., spin and parity) have been established yet. Evidence for both the $\psi' \to \gamma\eta_c$ ("hindered" M1) and the $J/\psi \to \gamma\eta_c$ ("allowed" M1) radiative decays has been observed. The quantitative rates, however, are quite poorly known, and there is the additional question of the total width of the η_c. New measurements of these quantities, with our increased data sets, will be presented in Sections II and III.

There remain two predicted charmonium bound states for which there is no substantial experimental evidence. One of these, the $^1P_1$ spin-singlet P-wave $c\bar{c}$ state, is supposed to have a mass equal to the center-of-gravity of the ^3P_J states [i.e., $m(^1P_1) \simeq 3520$ MeV]. The $^1P_1$ has negative charge conjugation parity, making the radiative decay $\psi' \to \gamma\,^1P_1$ forbidden. In addition, its parity is positive, ruling out the possibility of creating it directly in e^+e^- collisions via one photon annihilation. Thus, the $^1P_1$ is expected to be (as is evidently the case) very difficult to observe in e^+e^- collisions (and e^+e^- collisions are the cleanest place to study charmonium -- even the ^3P states are difficult to study in hadronic collisions). One chance to produce it is via the $\psi' \to \gamma\chi_2 \to \gamma\gamma\,^1P_1$ cascade, but the expected small $\chi_2 - ^1P_1$ splitting suppresses the rate, and the low energy photon complicates study. The similar cascade $\psi' \to \gamma\eta_c' \to \gamma\gamma\,^1P_1$, involving similar matrix elements (in reversed order), may have smaller or larger branching ratios, depending on the actual masses involved, and the relative total widths of the η_c' and χ_2 states. An intriguing possibility is the isospin-violating transition $\psi' \to \pi^o\,^1P_1$, which results in a low energy, monochromatic π^o (the $\psi' \to \pi^o\,^3P_J$,

$\psi' \to \pi^o\ ^1S_0$ transitions are forbidden by C-parity). The branching ratio for this S-wave decay could well be larger than the P-wave process $\psi' \to \pi^o\ J/\psi$ (BR $\approx$ 0.1%),[11] but there is a copious background from $\psi' \to \pi^o\pi^o\ J/\psi$ decays. On the other hand, the $^1P_1$ should have a very large branching fraction for the radiative decay to the η_c, so some suppression of background may be possible by looking for a monochromatic π^o in events which fit the $\psi' \to \gamma\pi^o\eta_c$ hypothesis. The other as yet unobserved $c\bar{c}$ bound state, the η_c', may not be as difficult to find. This state can be reached via an M1 radiative transition from the ψ'. A promising way to look for it is in the inclusive photon spectrum at the ψ', and evidence for such a transition will be presented in Sec. IV.

Finally, in addition to the radiative transitions between charmonium levels, there are three known hadronic transitions, all between the ψ' and J/ψ: (i) $\psi' \to \pi\pi\ J/\psi$, (ii) $\psi' \to \eta\ J/\psi$, and (iii) the isospin-forbidden decay $\psi' \to \pi^o\ J/\psi$. A natural question to ask is whether there are any other significant hadronic transitions. I will address this question in Section VI.

The Crystal Ball detector is a device which, in many ways, is uniquely suited to studying the transitions between $c\bar{c}$ bound states, and their radiative decays to other hadrons. Many details of this detector may be found elsewhere,[12] so I will only briefly review the more relevant characteristics. Figure 2 is a pictorial representation of the main components of the central detector. The essential idea of the Crystal Ball is the high resolution measurement of the energy and direction of electromagnetically showering particles over a large solid angle. This is achieved with the use of a segmented array of NaI(Tℓ) crystals (672 crystals covering 93% of 4π steradians in the central

DETECTOR COMPONENTS OF THE
CRYSTAL BALL-SLAC 1978

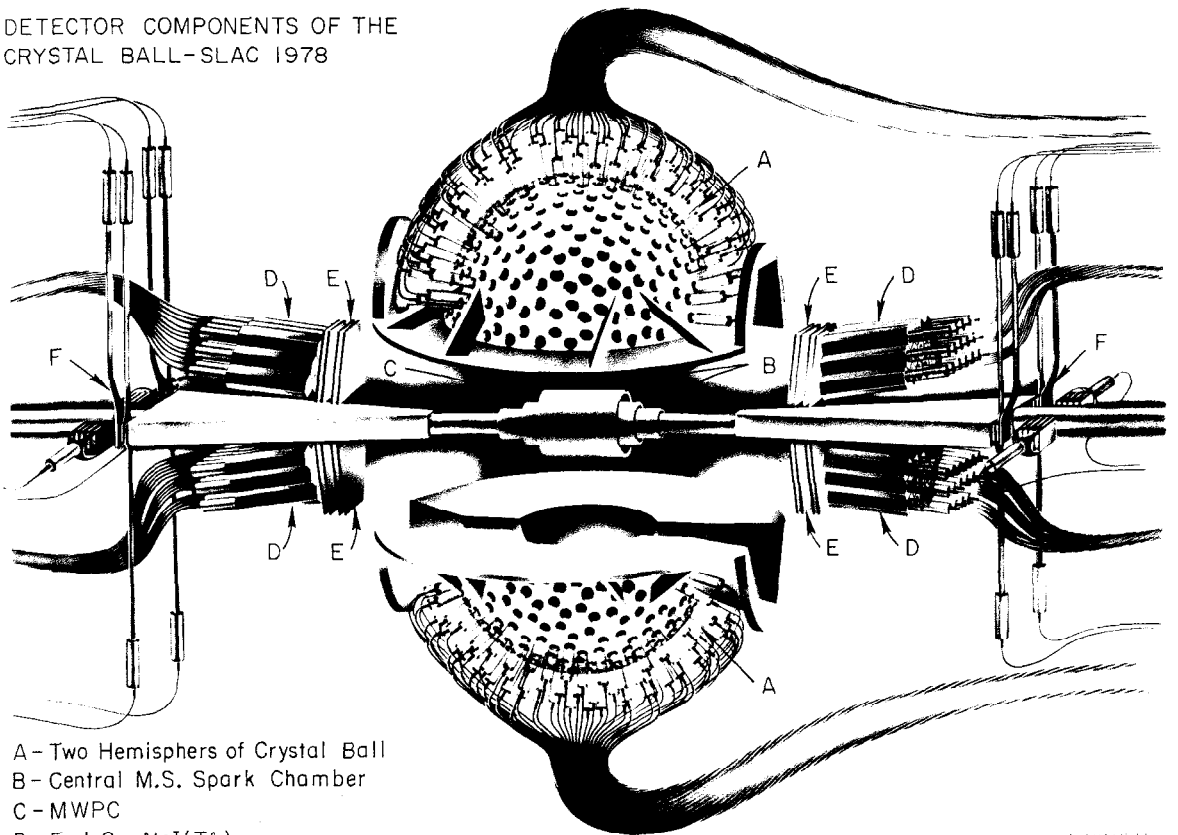

A - Two Hemisphers of Crystal Ball
B - Central M.S. Spark Chamber
C - MWPC
D - End Cap NaI(Tℓ)
E - End Cap M.S. Spark Chambers
F - Luminosity Monitor

5-79

3626A1

Fig 2.

detector, extended to 98% by an additional 60 crystals in the endcap regions), giving an energy resolution for photons and electrons of $\sigma_E/E \simeq 2.6\%/[E\ (GeV)]^{1/4}$ and an angular resolution of $1\text{-}2^o$ (slowly varying with energy). In addition, there are magnetostrictive-readout spark chambers and proportional wire chambers with cathode strip segmentation providing charged particle tracking and charged-neutral separation over the entire solid angle covered by the NaI. There is no magnetic field, so charged hadron energies are only poorly determined in the ~1 interaction length of NaI. A minimum ionizing particle deposits ~200 MeV (most probable energy loss) in the NaI.

II. INCLUSIVE PHOTON STUDY OF $\psi' \to \gamma\chi$ [13]

One of the goals of the Crystal Ball experiment has been to obtain precise measurements of the $\psi' \to \gamma\chi$ branching ratios by performing fits to the monochromatic lines in the inclusive photon spectrum for ψ' decays. Achieving this has required careful study of several aspects of the spectrum. Various cross checks on our understanding of these aspects have given us confidence in the results. Because of the complexity of the measurement, and because of the relevance to following sections of this report, I will describe the analysis and checks in some detail.

A. Event Selection

Events are selected from the available triggers on tape in order to suppress backgrounds from cosmic rays, beam-gas interactions, and QED events and to accept true hadronic decays of the J/ψ or ψ' resonances. The cuts employed for the data described here may be summarized as follows:

(a) Event must contain at least 3 tracks (a "track" may be neutral or charged) observed in the detector.

(b) The total observed energy, E_{tot}, must satisfy:

$$656 < E_{tot} < 3445 \text{ MeV} \quad \text{at} \quad J/\psi$$

$$800 < E_{tot} < 4100 \text{ MeV} \quad \text{at} \quad \psi'$$

(c) Remaining contamination from QED processes is reduced further by rejecting those events which have $E_{tot} > 0.35\ E_{c.m.}$ and satisfy:

(i) more than two tracks have $x \equiv E_{track}/E_{beam} > 0.5$ (E_{track} is the observed energy in the NaI); or

(ii) two tracks have $x > 0.5$, and the event only contains three observed tracks; or

(iii) one or two tracks have $x > 0.5$ and the total energy assigned to all other tracks, $E_{x < 0.5}$, is less than $0.06\ E_{c.m.}$; or

(iv) one or two tracks have $x > 0.5$ and $E_{x < 0.5} - E^{max}_{x < 0.5} < 0.02\ E_{c.m.}$, where $E^{max}_{x < 0.5}$ is the highest energy track with $x < 0.5$.

(d) Remaining contamination from cosmic rays and beam-gas collisions is suppressed further by a combination of requirements on the total energy observed and the symmetry of the energy deposition pattern:

(i) If the event satisfied the primary event triggers,[14] then an asymmetry parameter, A, is calculated for the event according to

$$A = \left| \sum_i E_i \hat{x}_i \right| / \sum_i E_i$$

where the sum is over the NaI crystals which contain $> 1/2$ MeV in deposited energy, and $\hat{x}_i$ is the unit vector pointing to the center of crystal i. The event is rejected if $A > 0.7$, or if the following relation is true:

$$E_{tot} < 0.2444\ E_{c.m.}\ [1 + (A/0.7)^{2.02}]\ .$$

(ii) For those events which did not satisfy one of the primary triggers, the simple requirement that $E_{tot} > 0.4\ E_{c.m.}$ was found to be suitable. This adds less than 1% to the selected event sample.

(e) In the ψ' data acquired during spring 1981 (slightly more than half the ψ' data), events which failed one or more of the above criteria were accepted anyway if it looked like they contained a $J/\psi \to \mu^+\mu^-$ or e^+e^- decay. This results in an increase of ~2% (mostly from $\psi' \to \pi\pi\ J/\psi \to \pi\pi\mu^+\mu^-$), and is done to facilitate the study of exclusive final states. It is largely irrelevant to the current inclusive results, but is mentioned for completeness.

The above criteria were developed by studying events from separated beam running ("empty target," permitting the investigation of beam-gas collisions), events which were not in-time with the e^+e^- beams crossing (dominated by cosmic rays), events which were in-time, and Monte Carlo simulated events. These criteria are optimized for the analysis of inclusive distributions, and the efficiency for accepting certain exclusive decays (e.g., $J/\psi \to \gamma\eta \to \gamma\gamma\gamma$) is significantly lower than the overall efficiency of 94%. The datasets used at the J/ψ and ψ' resonances are summarized in Table I.

TABLE I

J/ψ and ψ' Datasets

Resonance	$\int \mathscr{L}\, dt$ (nb^{-1})	Number of Events in Selected Sample[a]	Background Events in Sample[b]	Trigger and Selection Efficiency (±5%)	Number of Resonance Produced (±5%)
J/ψ	765	1779 K	24.5 K	0.94	2171 K
ψ'	3450	1752 K	75 K	0.94	1815 K

a. Note that the direct leptonic channels $e^+e^- \to J/\psi \to \ell^+\ell^-$ and $e^+e^- \to \psi' \to \ell^+\ell^-$ are excluded from this sample.

b. The background contamination is dominantly u,d,s physics. In addition, there is a residual contamination from beam-gas collisions and cosmic rays (0.5% at J/ψ, 1.2% at ψ').

B. Photon Selection

The selection of tracks for inclusive photon analysis has been done in various widely different ways so that the effects of the cuts and the background shapes on the resulting branching ratios can be checked. This study for the measurements of the $\psi' \to \gamma\chi_J$ rates was done with four spectra, shown in Figs. 3(a)-(d), which have successively tighter requirements on the particles:

(a) The first spectrum contains all particles, whether called charged or neutral by the offline analysis program, with only the requirement that $|\cos\theta| < 0.85$ (θ is the angle between the track and the incident positron direction). The solid angle cut insures that the track is in a region of the NaI where edge effects (from

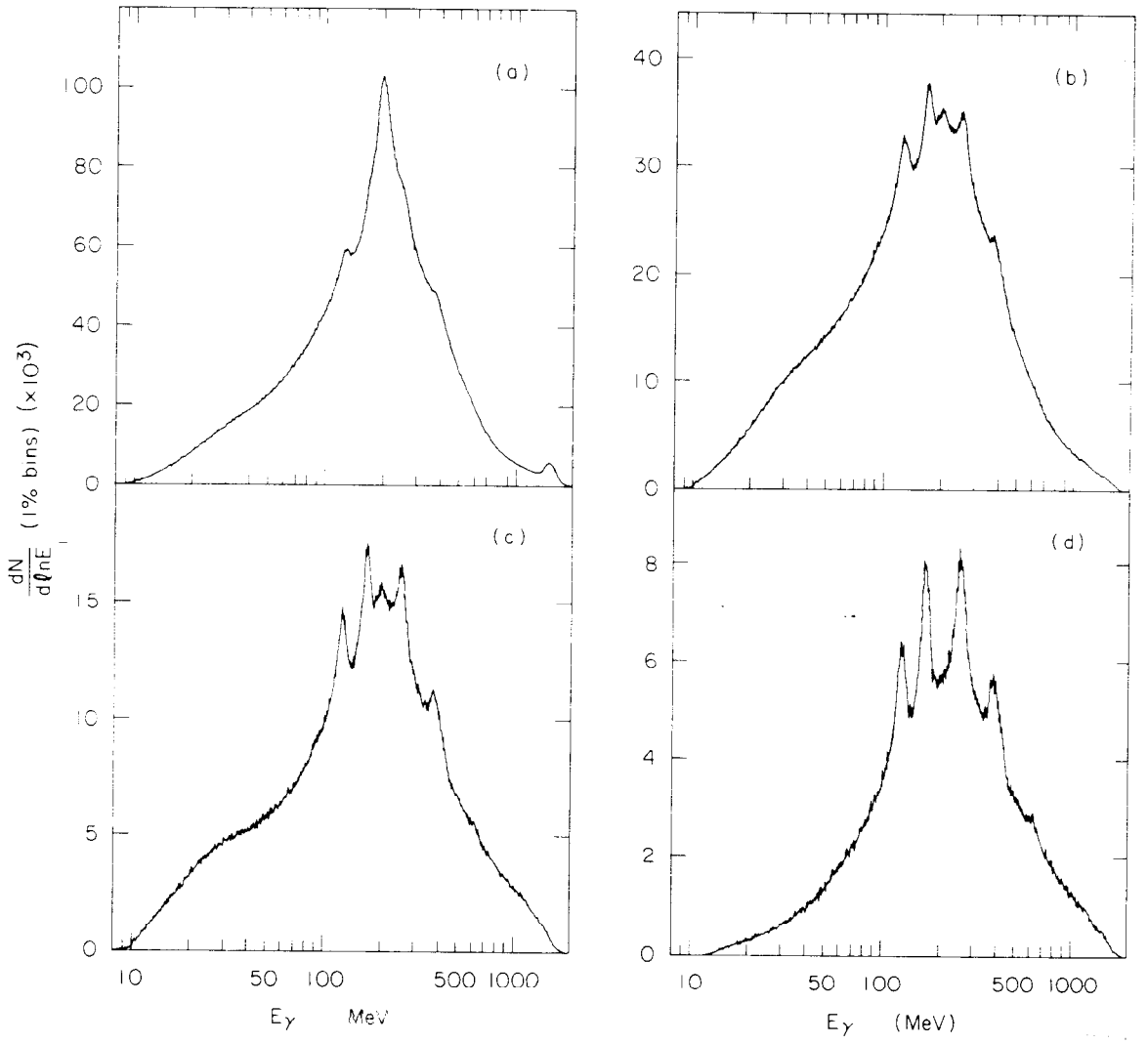

Fig. 3. Inclusive spectra at the ψ', used in the measurement of $BR(\psi' \to \gamma\chi_J)$ and $BR(\psi' \to \gamma\eta_c(2980))$. (a) All tracks, neutral and charged, with $|\cos\theta| < 0.85$; (b) same as (a), except neutrals only; (c) same as (b), except remove photons from π^0 decays and photons near interacting charged particles; and (d) same as (c), except require track to have a lateral shower pattern compatible with typical electromagnetically showering particles.

the beam-pipe tunnel regions) will not degrade resolution. This spectrum [Fig. 3(a)] has an enormous peak at ~200 MeV, corresponding to minimum ionizing charged particles passing through the detector. This peak dominates the spectrum, making the $\psi' \to \gamma\chi_J$ and $\chi_{2,1} \to \gamma\ J/\psi$ transitions appear only as shoulders. As we shall see, however, these shoulders are still highly significant and measurable.

(b) The second spectrum [Fig. 3(b)] contains the added selection that the tracks must be called neutral by the production analysis program. The large minimum-ionizing peak of Fig. 3(a) has almost disappeared to a small (but significant) bump due to charged particles which escape identification in the central chambers.

(c) The third spectrum [Fig. 3(c)] has two further requirements imposed on the particles: The dot product between the particle direction and the direction of any charged particle which interacts or showers in the NaI must be < 0.85; and photons which reconstruct to $\pi^o \to \gamma\gamma$ decays are removed.

(d) Finally, the fourth spectrum [Fig. 3(d)] contains only those tracks which also have a lateral shower energy deposition pattern in the NaI which is typical of a single photon shower. The minimum ionizing signal has vanished, the signal-to-background of the $\psi' \to \gamma\chi_J$ and $\chi_{1,2} \to \gamma\ J/\psi$ peaks has improved over the other spectra, and the $\psi' \to \gamma\eta_c$ transition is now clearly visible at $E_\gamma \sim 640$ MeV.

A parallel analysis is made on all four of these specta as a test of the sensitivity of the results to the cuts and background shapes.

C. Photon Detection Efficiency

The Crystal Ball detector itself is essentially 100% efficient for the detection of photons with energies $\gtrsim$ 1 MeV within our fiducial solid angle of $|\cos\theta| < 0.85$. However, the selection criteria and other effects reduce the efficiency with which photons will appear in our spectra. The resulting efficiency is calculated as a function of energy for each spectrum according to:

$$\varepsilon_\gamma = \varepsilon_{MC} f_\Omega \left(1 - \varepsilon_{conv}\right) \qquad (1)$$

where ε_{MC} is an efficiency calculated with a Monte Carlo technique (see below), f_Ω is a geometric correction factor for the photon angular distribution (assumed flat in the Monte Carlo calculation), and $\varepsilon_{conv} \simeq 0.028$ takes into account the probability that a photon will be called charged because of conversion in the beam-pipe or central chambers (not included in the Monte Carlo calculation). The largest correction for the angular distribution is for the $\psi' \to \gamma\chi_o$ decays, with a $1 + \cos^2\theta$ distribution, giving $f_\Omega = 0.79/0.85 = 0.93$.

The calculation of ε_{MC} is performed as follows: Photons of a specified energy are generated with a flat angular distribution, and propagated through the Crystal Ball detector geometry to produce showers using the EGS routines.[15] The resulting showers are then added to real J/ψ decay events, analyzed by the production analyses program, and these events are added to the real ψ' sample. The main assumption in this procedure is that the hadronic J/ψ decays are sufficiently similar to χ_J decays in such characteristics as multiplicity (see Sec. II-D, below for cross checks). A fit (for example, see Fig. 4; details of the

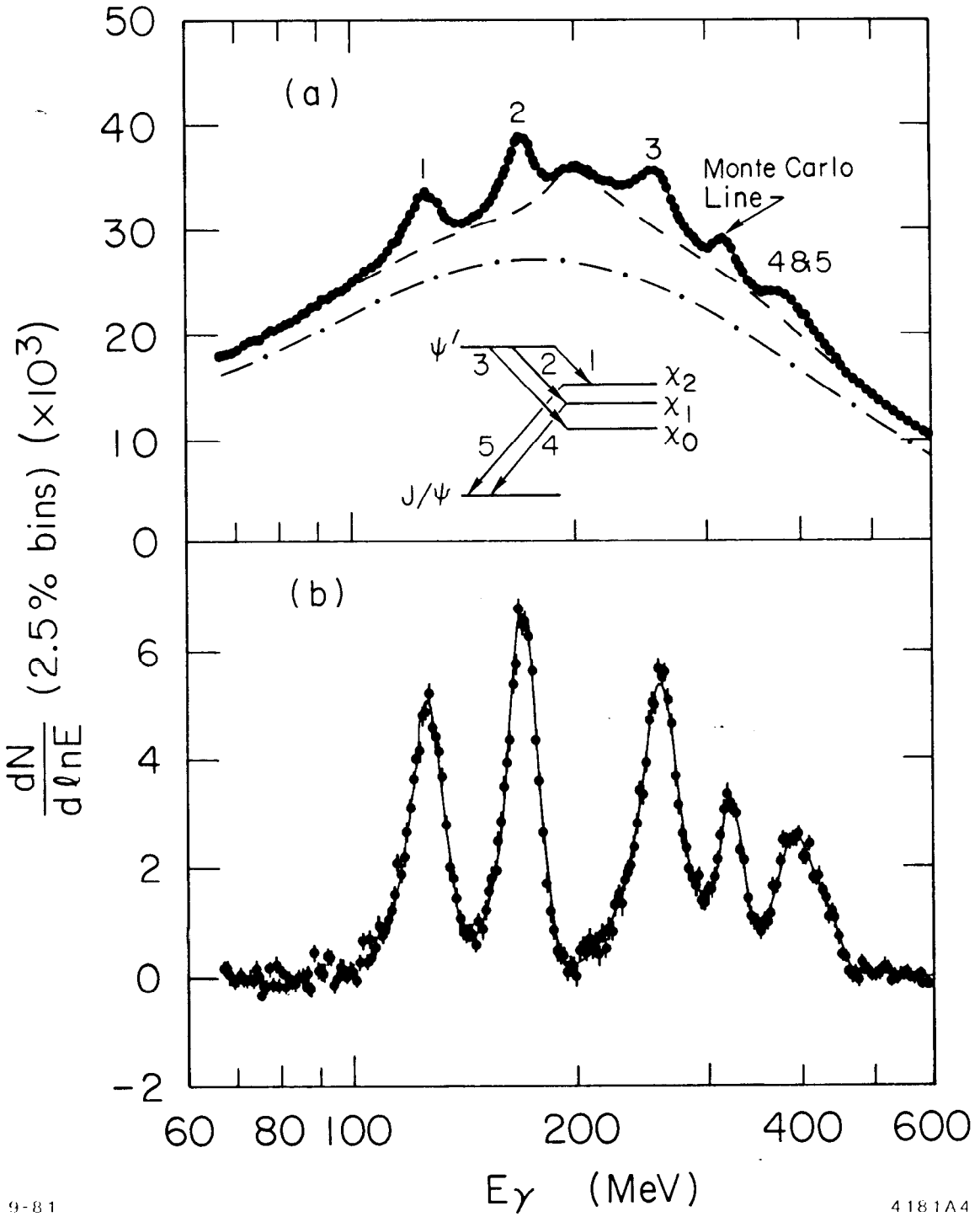

Fig. 4. An example of a fit to the inclusive photon spectrum [Fig. 3(b)] at the ψ' with an additional Monte Carlo transition added (see text) at 320 MeV: (a) before background subtraction. The background is indicated by the dashed curve passing under the peaks; the difference between the dashed and dot-dashed curves is the contamination from charged particles. (b) After background subtraction.

fits are described in Sec. II-D) is then made to the combined spectrum, and the size of the signal obtained for the Monte Carlo line is compared with the number generated. The resulting efficiencies (ε_{MC}) are shown as a function of energy and photon selection criteria in Fig. 5.

D. Fits to Inclusive Photon Spectra and Cross Checks

There are several factors involved in extracting reliable amplitudes and widths for the signals from the complicated spectra of Fig. 3. The shape of the signal itself depends on the shower characteristics in the detector, on the width of the recoil state, and on any dependence on the photon energy in the transition matrix element (to wide states). In addition, the background shape, which includes contributions from various sources, must be adequately modeled.

Studies of Bhabha events and the $\psi' \to \gamma\chi_1$ transition show that a reasonable line shape to use for monochromatic photons in the detector is a Gaussian with a power-law tail to low energies (joined with continuous first derivative). The energy resolution in the region of the γ transitions is assumed to obey the empirical $\sigma_E/E \propto 1/E^{1/4}$ function. The parameters of the line shape and resolution functions are determined with the $\psi' \to \gamma\chi_1$ inclusive photon signal, under the assumption that the χ_1 has an intrinsic width which is negligible compared with our resolution. This assumption is expected to be reasonable on theoretical grounds,[7] since the lowest-order perturbation theory decay of the χ_1 to hadrons is via 3 gluons. Experimentally, from the exclusive cascade channel analysis, we know that[12] $\Gamma(\chi_1) < 2.6$ MeV.

The χ_2 and χ_0 states are not assumed to be narrow, and a Breit-Wigner resonance shape is used, with width determined by the fits. In

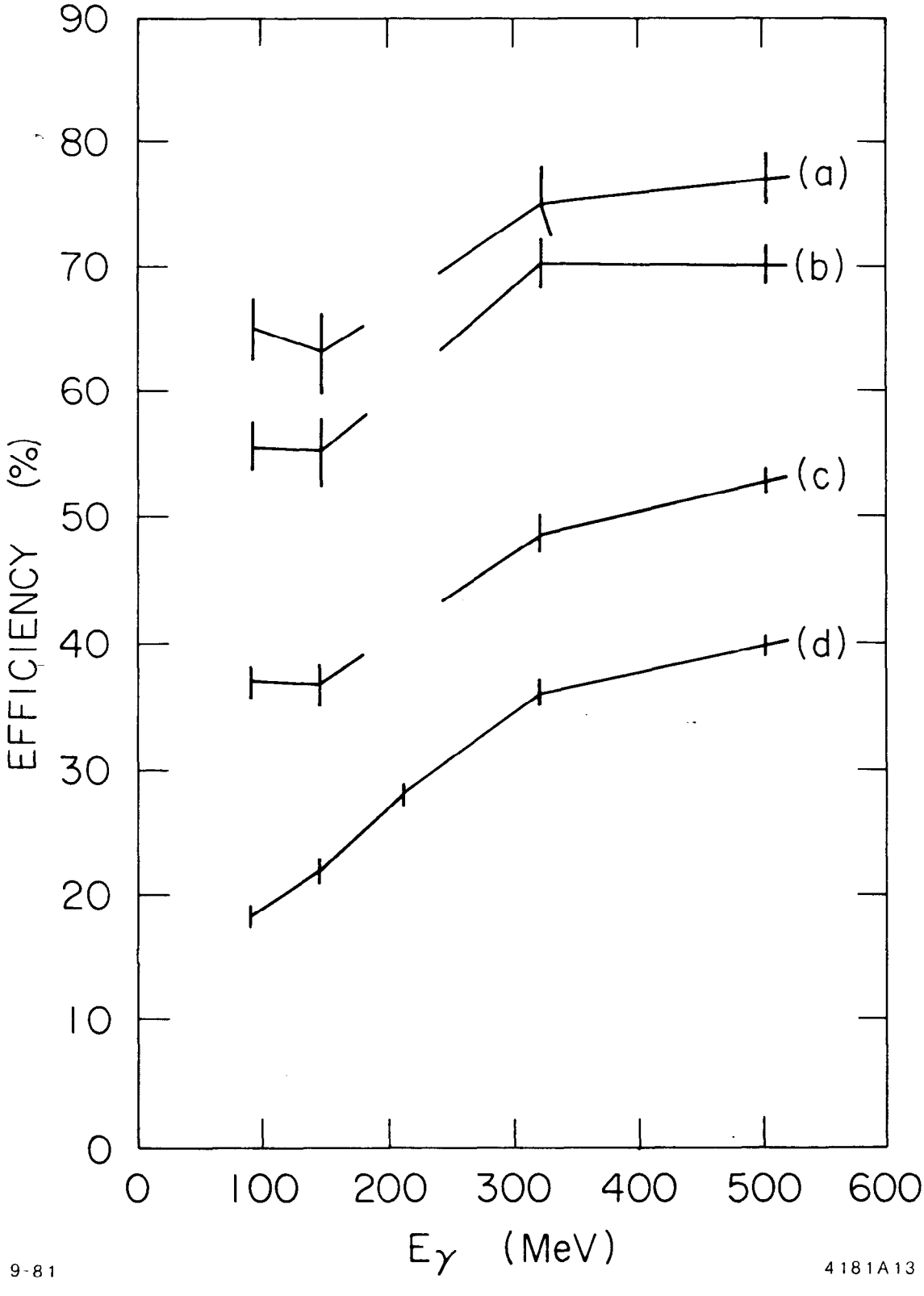

Fig. 5. Photon detection efficiencies as a function of energy for the different selection criteria. The letters correspond to the different spectra in Fig. 3. The region around 200 MeV for (a),(b) and (c) is complicated by the significant contamination from minimum ionizing charged particles.

addition, the transition matrix elements for these states is taken to be dominantly electric dipole.[12]

Background sources in the photon spectra are separated into three basic components:

(i) Contributions from charged particles. This source is included in the fits by measuring the shape of the charged particle spectrum (with cuts applied appropriate to the spectrum being fit) and including an amplitude for this shape in the fit [except for the fit to Fig. 3(d)].

(ii) Contributions from the decays $\psi' \to \eta\ J/\psi$ and $\psi' \to \pi^0\pi^0\ J/\psi$. The photons from these decays have limited phase space, so the fits include an amplitude for each of these shapes(only the η amplitude is found to be needed in the π^0-subtracted spectra), as determined by Monte Carlo calculation.

(iii) The remaining background is assumed to be smooth and is fit with a sum of Legendre polynomials (up to fifth order, if necessary).

Two examples of the final fits to the spectra are shown in Fig. 6 (see also Fig. 4). The Doppler-broadened $\chi_{1,2} \to \gamma\ J/\psi$ transitions are included in the fit, with mean fixed according to the $\psi' \to \gamma\chi_{1,2}$ results for the $\chi_{1,2}$ masses [and using $m(\psi') = 3684$ MeV, $m(J/\psi) = 3094$ MeV]. The χ^2 confidence levels for the fits are generally reasonable, a first sign that the lineshapes and backgrounds may be adequately modeled.

Two important cross checks that the determination of branching ratios from this analysis is under control are illustrated in Fig. 7. For each row of points in the figure, we can step through the results from the differently-selected spectra [Fig. 3(a)-(d)] by moving from

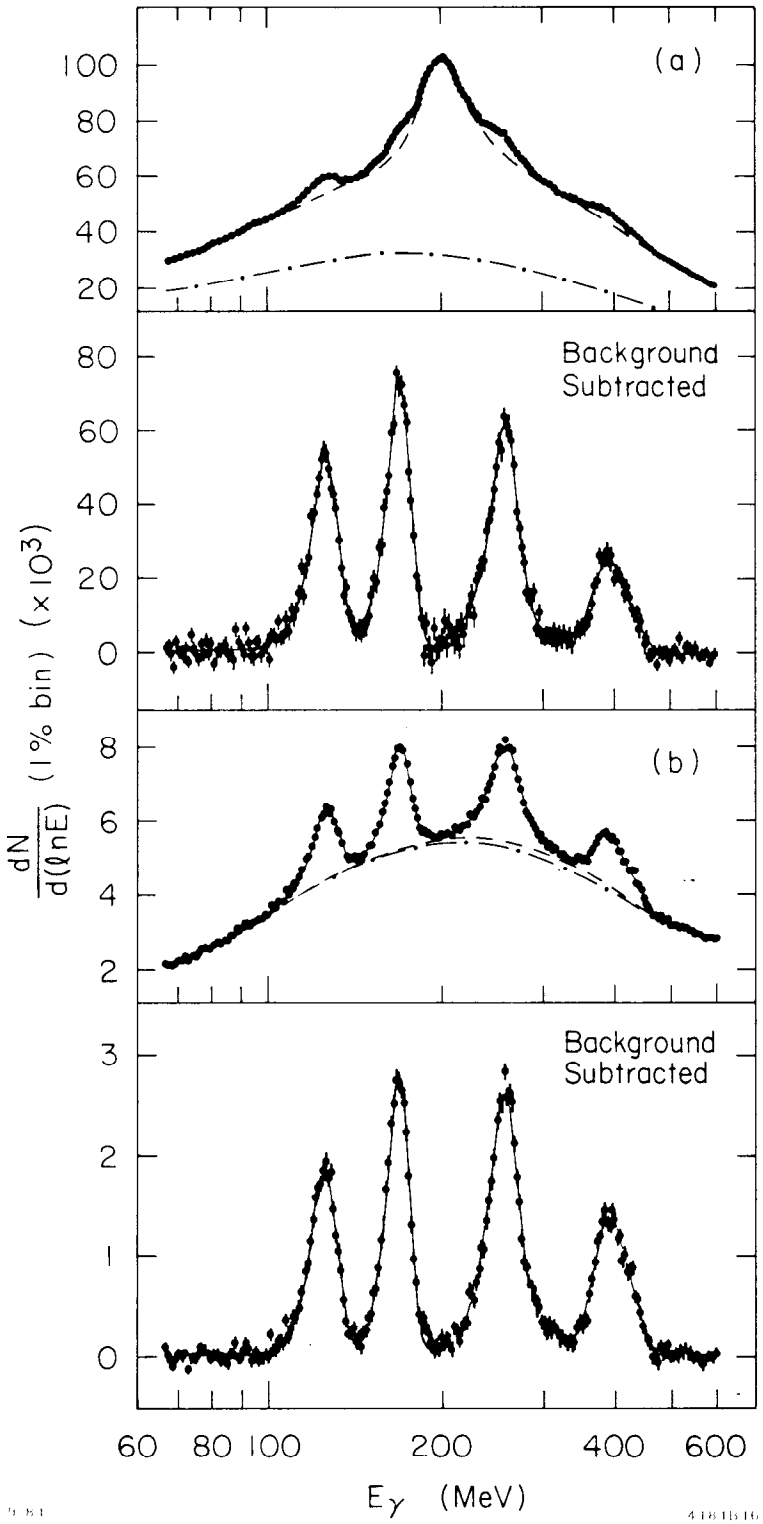

Fig. 6. Examples of fits to the ψ' inclusive photon spectrum. (a) is a fit to Fig. 3(a); and (b) a fit to Fig. 3(d). The background is indicated by the dashed curves. The difference between the dashed and dot-dashed curves is the contribution from charged particles plus $\psi' \to \eta J/\psi$ and $\psi' \to \pi^0\pi^0 J/\psi$ in spectrum (a), and from $\psi' \to \eta\, J/\psi$ in spectrum (b).

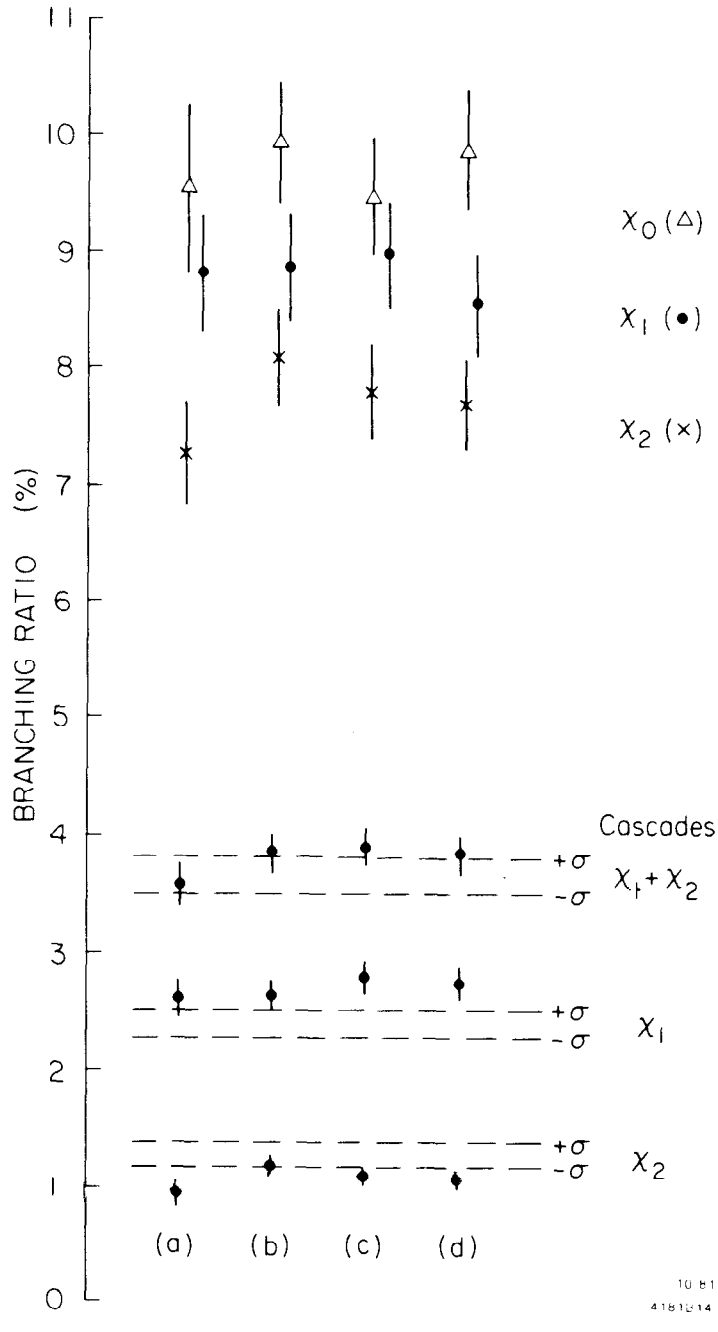

Fig. 7. Cross checks on the extraction of branching ratios from the ψ' inclusive photon spectra. The (a), (b), (c) and (d) designations refer to the differently selected spectra shown in Fig. 3. The points in the top half of the figure are the branching ratios for the $\psi' \to \gamma\chi_J$ transitions. The points in the bottom half are the branching ratios obtained (from the inclusive spectra) for the cascade process: $\psi' \to \gamma\chi_J \to \gamma\gamma\, J/\psi$. For comparison, the ±1 standard deviation (statistical only) intervals are shown from the Crystal Ball measurement of the cascade process in the exclusive channel: $\psi' \to \gamma\chi_J \to \gamma\gamma\, J/\psi \to \gamma\gamma\ell^+\ell^-$ ($\ell = \mu$ or e).

left to right. The fact that consistent results are obtained with such widely different background shapes [even Fig. 3(a)!] gives us confidence in this procedure for the extraction of branching ratios. The second check is the comparison of the product branching ratios $BR(\psi' \to \gamma\chi_{1,2})$ $\cdot$ $BR(\chi_{1,2} \to \gamma\ J/\psi)$ as measured with the Doppler-broadened secondary transition lines in the inclusive spectra with the measurement of the same quantities using the Crystal Ball in the exclusive channel[12] $\psi' \to \gamma\gamma\ J/\psi$, $J/\psi \to e^+e^-$ or $\mu^+\mu^-$. The inclusive measurement for the χ_2 is somewhat lower than the exclusive measurement, while for the χ_1 it is somewhat higher. Taking the sum of the two states yields agreement between the two measurements. This observed effect is easily understood, and has been verified with a Monte Carlo calculation. The point is that when a stronger transition ($\psi' \to \gamma\chi_1 \to \gamma\gamma\ J/\psi$) is strongly overlapped with a weaker transition ($\psi' \to \gamma\chi_2 \to \gamma\gamma\ J/\psi$), the fits become biased such that the stronger transition "steals" signal from the weaker. The fact that the sum is in agreement with the exclusive measurement allows us to say that the uncertainty in the absolute normalization of the inclusive results is $\lesssim$ 16%, the absolute error in the exclusive measurement[12] [which is dominated by the uncertainty in $BR(J/\psi \to e^+e^-$ or $\mu^+\mu^-)$].

E. Results for $\psi' \to \gamma\chi_J$

Table II summarizes the results obtained with the inclusive photon measurements for $\psi' \to \gamma\chi_J$, and gives an indication of how these results compare with theory. Space prohibits a review of the various model predictions, so I have emphasized only the coupled channel model of Ref. 8. While the $\psi' \to \gamma\chi_J$ branching ratios are slightly higher than

TABLE II

Results from $\psi' \to \gamma\chi_J$

DATUM	χ_0	χ_1	χ_2
$BR(\psi' \to \gamma\chi_J)$			
Crystal Ball[a]	0.097 ± 0.006 ± 0.016	0.088 ± 0.005 ± 0.014	0.077 ± 0.005 ± 0.012
SP-27	0.072 ± 0.023	0.071 ± 0.019	0.070 ± 0.020
Coupled Channel Model[b]	0.20 ± 0.04	0.158 ± 0.029	0.110 ± 0.021
Relative Rates[c]			
Crystal Ball	1.00 ± 0.07	1.05 ± 0.08	1.37 ± 0.09
E1 Theory	1	1	1
With OCD Corrections[d]	1	1.5	1.7
$\Gamma_{tot}(\chi_J)$ (MeV)			
Crystal Ball[e]	16 ± 4	< 2.6 90% C.L. (Assumed 0)	2 ± 1
$BR(\psi' \to \gamma\chi_J \to \gamma\gamma\ J/\psi)$ (%)			
Crystal Ball (Ref. 12)[a]	0.059 ± 0.015 ± 0.009	2.38 ± 0.12 ± 0.38	1.26 ± 0.08 ± 0.20
$\Gamma(\chi_J \to \gamma\ J/\psi)$ (KeV)			
Crystal Ball	97 ± 38	< 700	330 ± 170
Coupled Channel Model[b]	130	257	350

(a) First error is point-to-point, second is systematic normalization uncertainty.

(b) Reference 8. The uncertainty is from the experimental uncertainty in $\Gamma_{tot}(\psi')$.

(c) Proportional to $\Gamma(\psi' \to \gamma\chi_J)/(2J+1)E_\gamma^3$.

(d) Reference 16. I have used their result with the parameters of Ref. 8.

(e) Limit on $\Gamma(\chi_1)$ from Ref. 12. The χ_0 and χ_2 widths are obtained under the assumption that the χ_1 width is zero. Pending further analysis, these widths must be considered preliminary.

the results reported by the SP-27 experiment,[6] they are still substantially lower than the prediction of the model, assuming electric dipole (E1) dominance. The prediction depends on the wave functions, and there is also the possibility that relativistic or QCD corrections may be significant. In any event, an understanding of the discrepancy should be illuminating.[34]

Assuming E1 dominance, the relative rates for the $\psi' \to \gamma\chi_J$ decays do not depend on the details of the wave functions, and the quantity $\Gamma(\psi' \to \gamma\chi_J)/[(2J+1)E_\gamma^3]$ should be the same for all three transitions. We see that this is approximately the case experimentally (see Table II). First-order QCD corrections to the simple E1 prediction, involving gluon exchange, have been calculated.[16] It is encouraging that these corrections are in the right direction, but they are too large. Perhaps the model dependences in the corrections could account for some of this, or maybe higher-order corrections are not really negligible.

The prediction of the total widths for the χ states is rather model dependent, but a simple prediction for the relative widths of the χ_2 and χ_0 exists which depends only on the gluon-counting picture[7,17] (see Ref. 17 for first-order corrections):

$$\frac{\Gamma(\chi_2 \to \text{hadrons})}{\Gamma(\chi_0 \to \text{hadrons})} = \frac{4}{15} = 0.267 \ . \qquad (2)$$

Neglecting the non-hadronic decays, our preliminary inclusive measurement gives 0.13 ± 0.07. Subtracting the radiative widths will make the number smaller. However, the experimental measurement of the χ_2 width depends critically on the assumption that the χ_1 width can be neglected.

Also, a measurement of the χ_2 width using the exclusive $\psi' \to \gamma\chi_2 \to \gamma\gamma\ J/\psi \to \gamma\gamma\ell^+\ell^-$ channel gave a somewhat larger width[12] $\Gamma_{tot}(\chi_2) = 4.1 \pm 0.9$ MeV. Thus, a definitive comparison with theory must await some additional understanding of the subtleties involved in measuring the width (studies of which are in progress).

The radiative width for $\chi_J \to \gamma\ J/\psi$ is estimated according to:

$$\Gamma(\chi_J \to \gamma\ J/\psi) = \frac{BR(\psi' \to \gamma\chi_J \to \gamma\gamma\ J/\psi)}{BR(\psi' \to \gamma\chi_J)} \Gamma_{tot}(\chi_J) \cdot \qquad (3)$$

The results (Table II) are, in this case, compatible with the absolute prediction of the coupled channel model, although the error bars are large.

III. $\psi' \to \gamma\eta_c$ and $J/\psi \to \gamma\eta_c$

With the doubling of both the ψ' and the J/ψ datasets in the past year, we have repeated and refined the analysis of the inclusive photon spectra for the radiative transitions to the η_c candidate state observed earlier.[9,10] The approach is very similar to that described in Sec. II for the $\psi' \to \gamma\chi_J$ analysis, using spectra with a variety of photon selection criteria to evaluate the sensitivity of the results to the cuts and background shape. The detailed cuts are the same as those shown for the ψ' [Figs. 3(a)-(d)], except that the lateral shower pattern cut is broken into two steps. The first step rejects shower patterns which are too broad, reducing contamination from high-energy (> 600 MeV) π^o's with merged showers from the decay γ's, and from hadronic showers. The second step eliminates shower patterns which are

too narrow, suppressing the remaining contribution from minimum ionizing charged particles which escape identification by the central chambers. The five spectra, corresponding to the five steps in the selection criteria are shown for the J/ψ data in Fig. 8. The ψ' spectra shown in Figs. 3(a)-(d) have the same cuts applied as for the J/ψ spectra of Figs. 8(a),(b),(c) and (e), respectively.

For each set of cuts, the procedure is to make a simultaneous fit to both the J/ψ and ψ' inclusive photon spectra for the radiative transition to the η_c, constraining the η_c mass and width to be the same for both spectra. An example of such a fit is shown in Fig. 9. The photon detection efficiencies are estimated similarly to the estimates in Sec. II-C, under the assumption the η_c decays are similar in general features to the hadronic J/ψ decays.

The analysis is very similar to that described in Sec. II. The results of the fits to the different spectra are compared as a consistency check. An additional check is made by comparing the mass and width obtained from the spectrum for events containing exactly two observed charged particles. The results are as follows:[18]

(i) $m_{\eta_c} = 2984 \pm 2(\text{statistical}) \pm 4(\text{systematic})$ MeV. The 1^3S_1-1^1S_0 hyperfine splitting is thus 111 ± 5 MeV.

(ii) $BR(J/\psi \to \gamma\eta_c) = \left(1.20 \begin{smallmatrix} + 0.53 \\ - 0.35 \end{smallmatrix}\right)\%$. This may be compared with the prediction based on the assumption that it is an M1 allowed transition:[8]

$$\Gamma(n^3S_1 \to \gamma + n^1S_0) = \frac{16}{3}\left(\frac{Q}{2m_c}\right)^2 \alpha E_\gamma^3$$

$$= 1275\,[E_\gamma\ (\text{GeV})]^3\ \text{keV} \qquad (4)$$

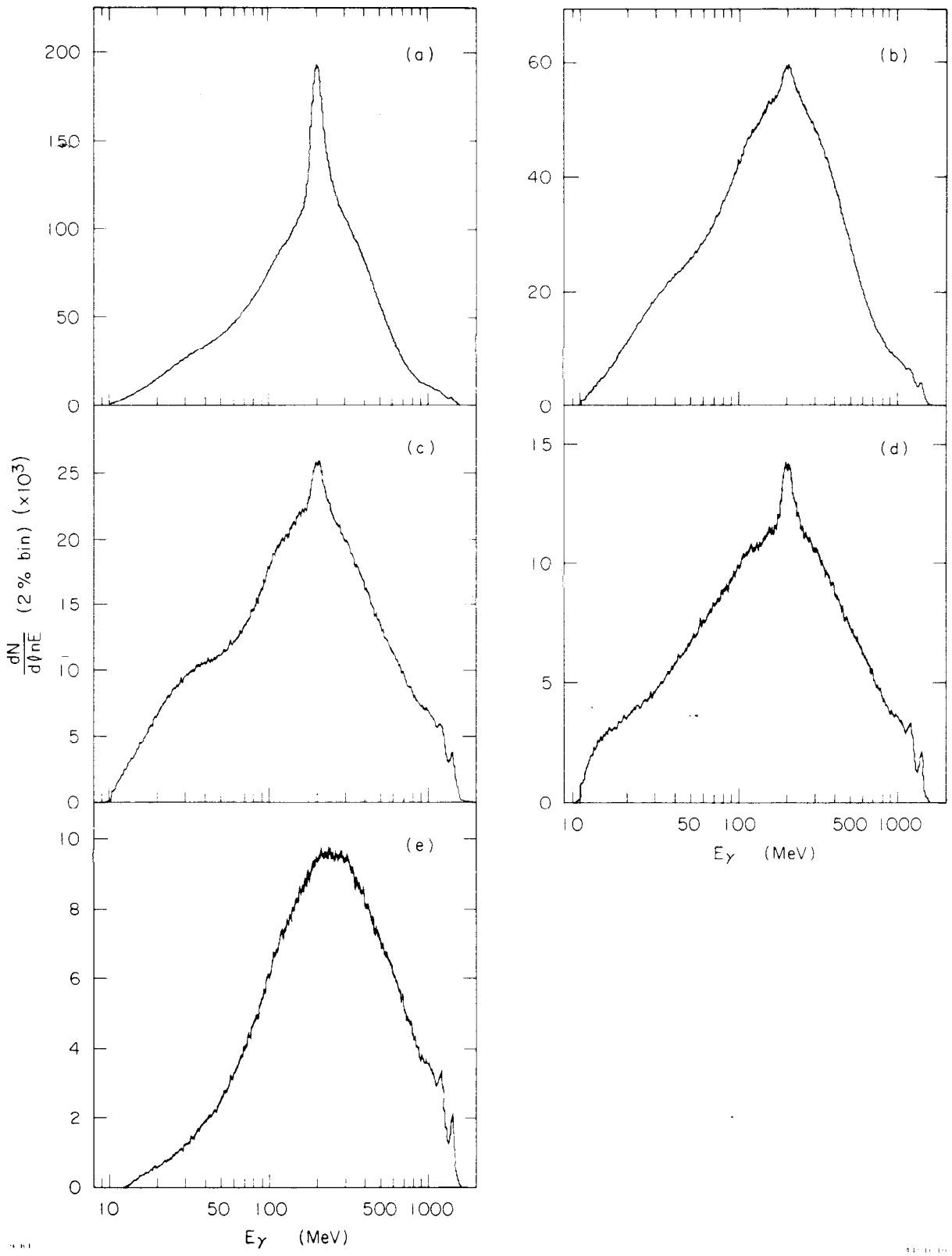

Fig. 8. Inclusive spectra at the J/ψ, used in the measurement of the J/$\psi \to \gamma\eta$ transitions. Spectra (a), (b), (c) and (e) are made with the same selection criteria as Fig. 3(a),(b),(c),(d),respectively, at the ψ'. Part (d) includes the part of the lateral shower pattern cut which eliminates showers which are too broad (e.g., from the merged showers of two photons), but not the cut which eliminates too narrow showers (e.g., from minimum ionizing charged particles).

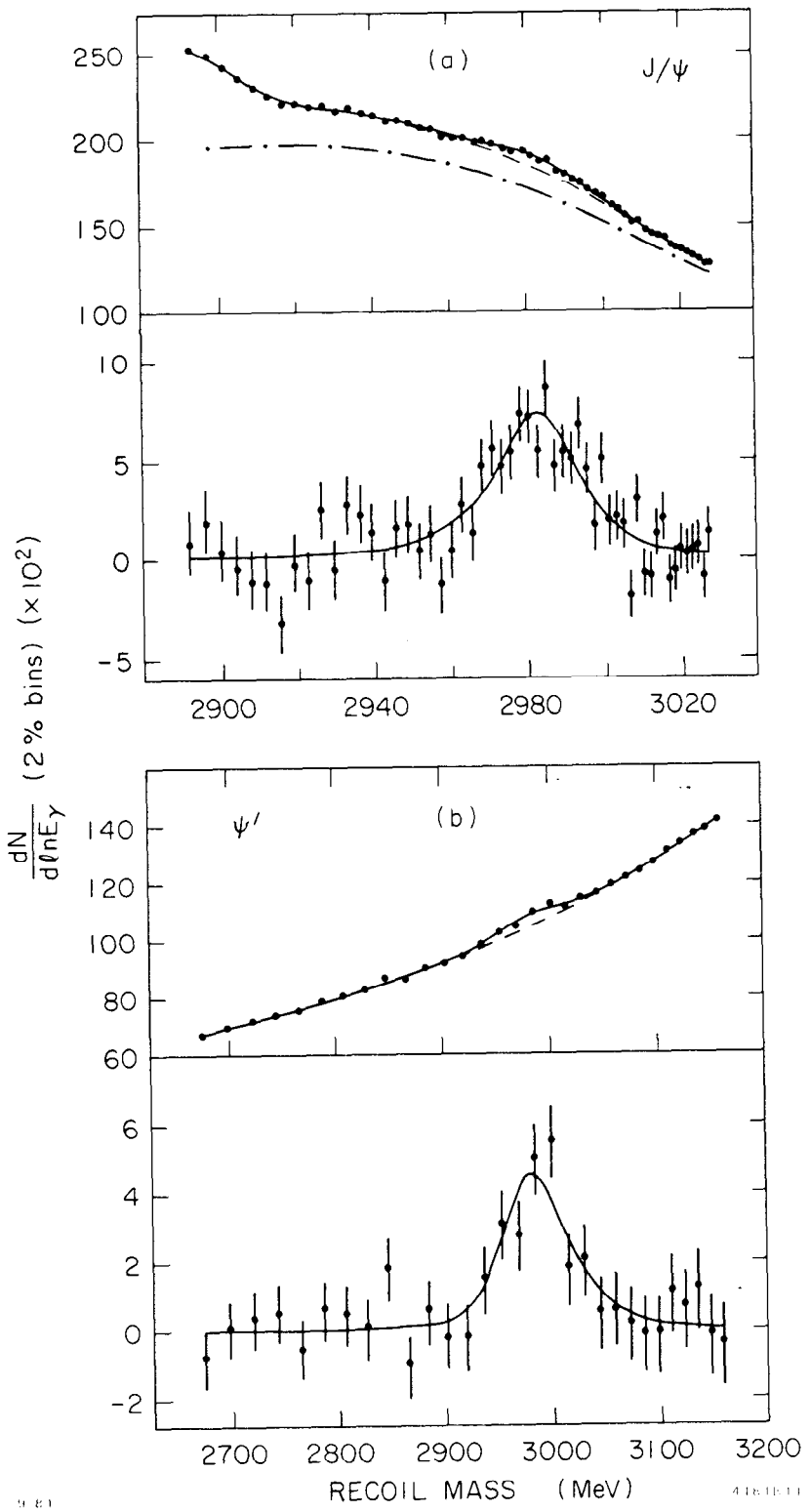

Fig. 9. An example of a simultaneous fit to the J/ψ(a) and ψ'(b) inclusive photon spectra for the radiative decay to the η. The spectra shown here are from Figs. 3(c) and 8(c). The difference between the dot-dashed and dashed curves in (a) is the background contamination from misidentified charged particles.

where Q = 2/3 is the quark charge, and m_c = 1.84 is the charmed quark mass. Putting into this formula the observed E_γ, and dividing by the J/ψ total width, we find: $BR(J/\psi \to \gamma\eta_c)$ = (2.6 ± 0.5)%. As with the $J/\psi \to \gamma\chi_J$ transitions, there is thus an indication that the rate is smaller than the simple expectation.

(iii) $BR(\psi' \to \gamma\eta_c)$ = (0.29 ± 0.08)%. This is a "hindered" M1 transition, and the theoretical estimates depend on the details of the two different radial wave functions. Scaling the prediction of Ref. 8 ("naive model") to the observed value for the splitting [Γ(hindered M1) $\propto E_\gamma^7$, approximately], we expect $BR(\psi' \to \gamma\eta_c)$ = (0.45 ± 0.09)%, where the error is from the uncertainty in $\Gamma_{tot}(\psi')$ and E_γ.

(iv) $\Gamma_{tot}(\eta_c)$ = 12.4 ± 4.6 MeV. A prediction for this width may be obtained using the measured J/ψ width to eliminate the dependence on wave functions, and using the lowest-order gluon-counting:[7]

$$\frac{\Gamma(J/\psi \to ggg)}{\Gamma(\eta_c \to gg)} = \alpha_s \left[\frac{5(\pi^2 - 9)}{27\pi} \right] \qquad (5)$$

For α_s = 0.2 and $\Gamma(\psi \to \text{hadrons})$ = 54 ± 9 KeV, this gives $\Gamma(\eta_c \to \text{hadrons})$ = 5.3 ± 0.9 MeV. The next-order QCD corrections to this are in the direction to make it larger, and are likely to be substantial.[19]

In addition to the inclusive photon analysis of $J/\psi, \psi' \to \gamma\eta_c$, we have repeated the search for $\eta_c \to \gamma\gamma$ in the $J/\psi \to \gamma\gamma\gamma$ channel[20] with the doubled data set. Figure 10 shows the gamma-gamma mass distribution in

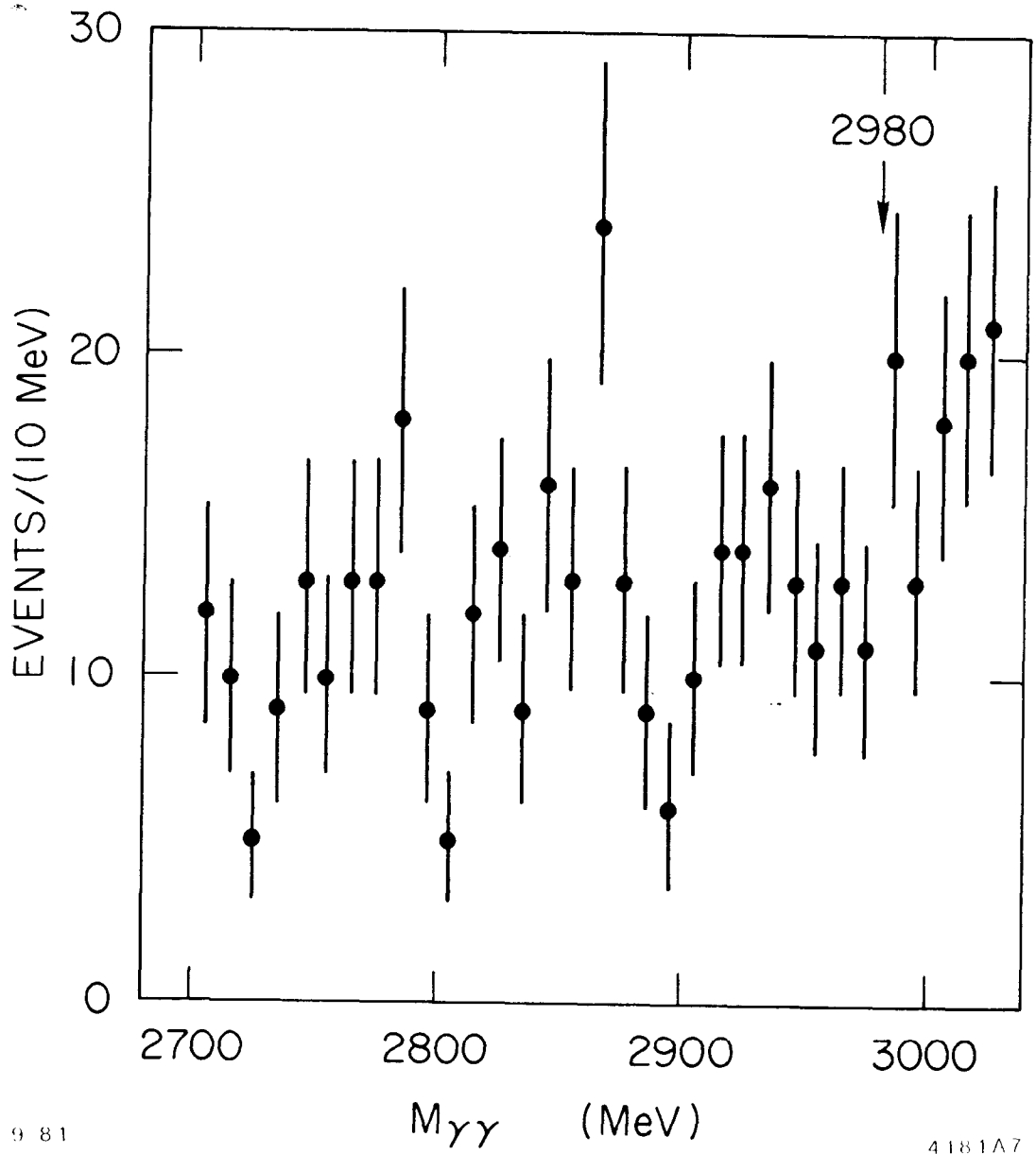

Fig. 10. The gamma-gamma mass distribution in the high mass region for events which fit the hypothesis $J/\psi \to 3\gamma$. The resolution is such that a signal for a zero-width state would be mostly contained within two bins.

the high-mass region for events fitting $e^+e^- \to \gamma\gamma\gamma$ at $E_{c.m.} = m(J/\psi)$. There is no significant signal observed above the background from QED events and $J/\psi \to \gamma\eta$, $\gamma\eta'$ decays. Thus we set a limit for the product of branching ratios:

$$BR(J/\psi \to \gamma\eta_c(2.98) \to \gamma\gamma\gamma) < 1.6 \times 10^{-5} \quad 90\% \text{ C.L.} .$$

Dividing out the measured $J/\psi \to \gamma\eta_c$ branching ratio, and multiplying by the observed total width, this means that $\Gamma(\eta_c \to \gamma\gamma) < \sim 20$ keV. A simple prediction for this quantity may be obtained by using the known $J/\psi \to \mu^+\mu^-$ rate to remove the wave function dependence in the result of the QED calculation for the decay:[7,18]

$$\Gamma(\eta_c \to \gamma\gamma) = \Gamma(J/\psi \to \mu^+\mu^-)\ 3\left(\frac{2}{3}\right)^2$$

$$= 6.3 \pm 0.7 \text{ keV} . \qquad (6)$$

This is comfortably below our upper limit.

IV. EVIDENCE FOR AN η_c' CANDIDATE STATE

As mentioned in the introduction, a reasonable way to search for the predicted 2^1S_0 radial excitation of the η_c, the η_c', is to look in the inclusive photon spectrum at the ψ' for evidence of the $\psi' \to \gamma\eta_c'$ decay. In this section, I describe such evidence observed for a state at a mass 3592 ± 5 MeV.

The event selection for this analysis is the same as described in Sec. II-A, with the minor additional rejection of events with more than 10 charged or more than 10 neutral observed tracks. The photon selection criteria are as follows:

(a) The track must be identified as neutral by the Crystal Ball offline analysis program.

(b) $|\cos\theta| < 0.85$.

(c) $\cos\theta_{\gamma\cdot\text{charged}} < 0.90$, where $\theta_{\gamma\cdot\text{charged}}$ is the opening angle between the neutral and the nearest charged track.

(d) The lateral shower energy deposition pattern in the NaI must be typical of a single photon shower. (The details of this cut are slightly different than the one used in Secs. II and III.)

The effect of criterion (d) on charged particles may be seen in Fig. 11(a). The second peak at ~1500 MeV is due to $J/\psi \to e^+e^-$ decays. Note that the pattern cut has very little effect on this peak, as it is due to electromagnetically showering particles.

The ψ' inclusive photon energy spectrum after the above selection is shown in Fig. 11(b). For comparison, Fig. 11(c) shows the corresponding spectrum for J/ψ decays. The most prominent features in Fig. 11(b) are the three monochromatic photon peaks from the $\psi' \to \gamma\chi_{2,1,0}$ transitions, and a peak due to the overlapping contributions from the two Doppler-broadened transitions $\chi_2 \to \gamma\ J/\psi$ and $\chi_1 \to \gamma\ J/\psi$. In addition to these peaks (and a residual contamination from misidentified charged particles), there are two other statistically significant, but much less obvious features in the spectrum.[21] One of these is at a photon energy of about 640 MeV, corresponding to a recoil mass of 2980

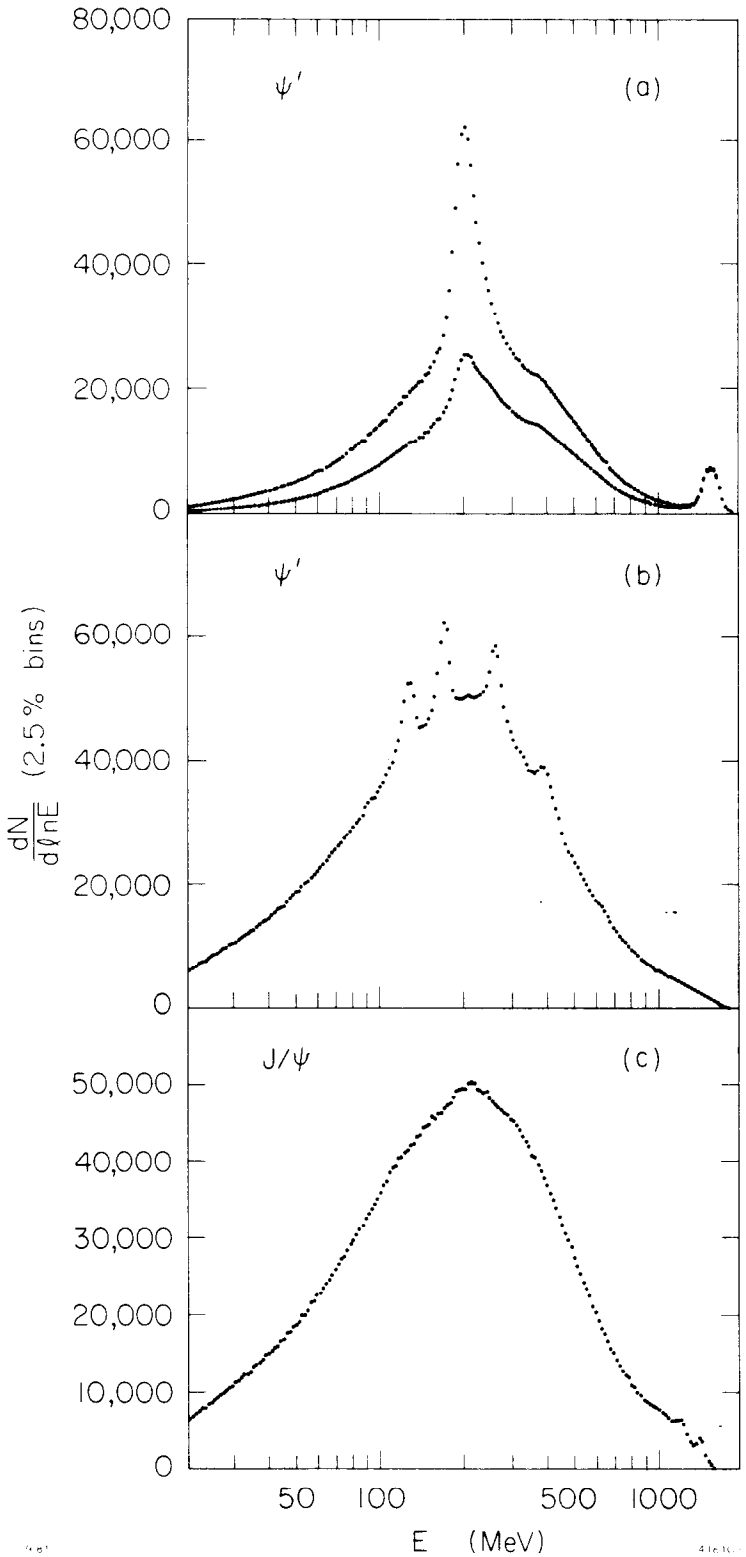

Fig. 11. Inclusive particle observed energy spectra at the ψ' and J/ψ with cuts described in text. (a) Observed energy for well-identified charged tracks at the ψ'. The upper points are before the application of a cut on the lateral shower pattern, the lower points are after this cut. (b) The inclusive photon energy spectrum for ψ' decays, used in the search for $\psi' \to \gamma\eta'$. (c) The inclusive photon energy spectrum at the J/ψ, with identical selection as in (b).

MeV, the presumed η_c. A fit to this structure with a smooth background (sum of Legendre polynomials) plus a peak with resolution width yields a signal strength of 2826 ± 404 photons and a photon energy of 638 ± 4 MeV (statistical error only). The remaining structure appears at a photon energy of approximately 90 MeV, and we shall now consider this in more detail.

Figure 12 shows the result of performing a fit to the region containing the 90 MeV structure. A smooth background in the form of a sum of Legendre polynomials up to cubic order was assumed, plus a signal term with resolution width. This fit yields a signal amplitude of 5582 ± 1270 photons, with a mean energy of 90.8 ± 0.8 MeV. Both the signal (mean and amplitude) and the background shape were allowed to vary simultaneously. If, instead, we fix the background shape as determined by fitting to the region excluding the signal, consistent results are obtained, but the statistical significance of the signal improves (to > 6 standard deviations). Additional fits made to study the width of the state recoiling against the photon give a result which is consistent with zero width and a 95% C.L. upper limit of $\Gamma < 8$ MeV. Considering the systematic uncertainty in the photon energy (including the absolute energy calibration uncertainty and a small correlation with Γ), the mean energy is 91 ± 5 MeV, corresponding to a recoil mass of 3592 ± 5 MeV (assuming $M_{\psi'} = 3684$ MeV). The width and signal strength are correlated, making a precise branching ratio determination difficult. Including this source of uncertainty, and correcting for the photon detection efficiency (0.44 ± 0.08), we obtain a 95% confidence interval for the branching ratio: $BR(\psi' \to \gamma + 3592) = (0.2 - 1.3)\%$.

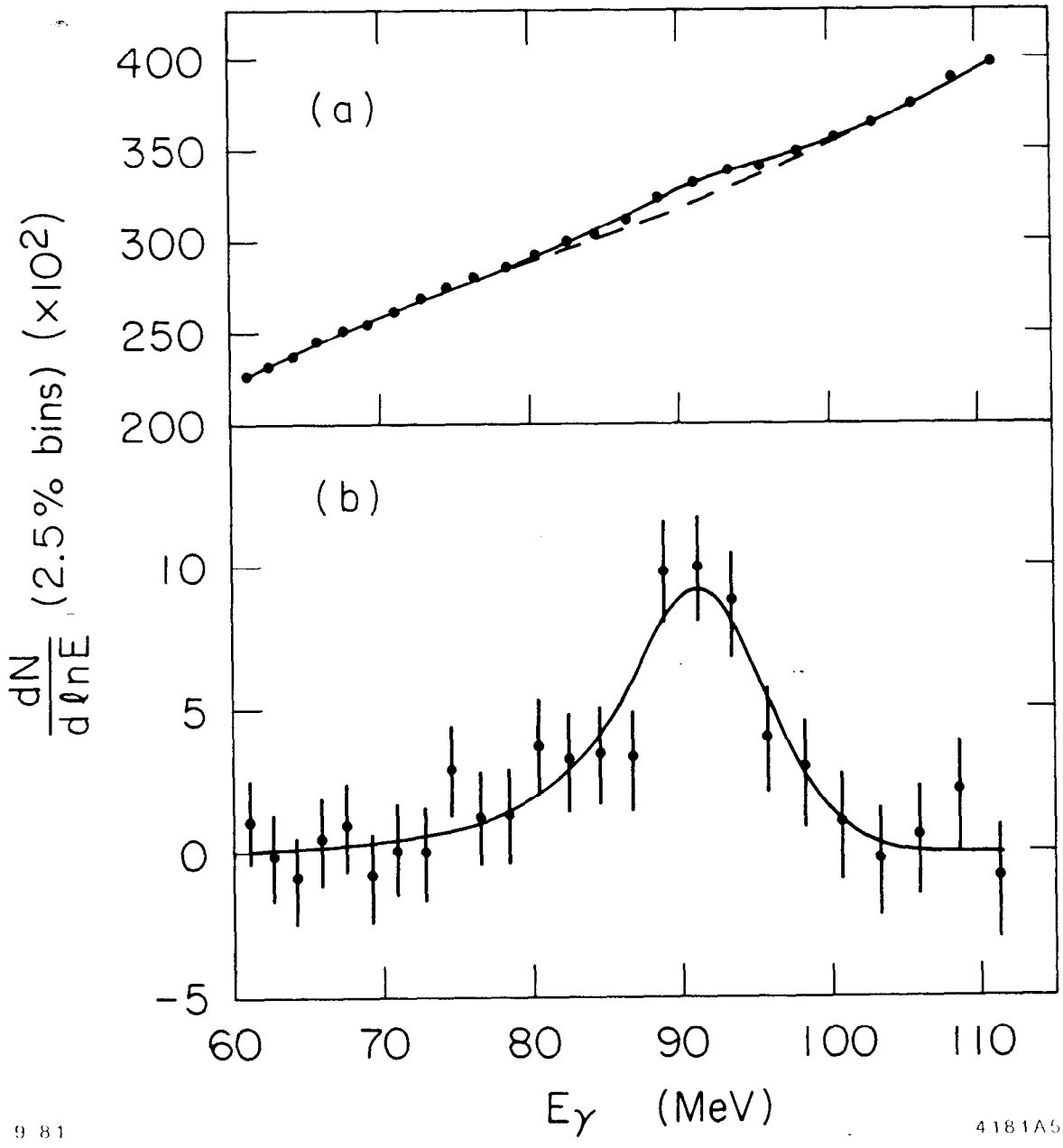

Fig. 12. A fit to the region around 90 MeV of the ψ' photon spectrum shown in Fig. 11(b): (a) Before background subtraction. The dashed line indicates the background contribution. (b) After background subtraction.

We have considered, and ruled out, several possible sources for the signal other than the interesting one that it indicates a new particle:

(i) The possibility that the signal is due to misidentified charged particles is eliminated by the absence of structure at 90 MeV in the charged particle observed-energy spectrum [Fig. 11(a)].

(ii) There are exclusive ψ' decays, such as $\psi' \to \pi^o\pi^o$ J/ψ and $\psi' \to \eta$ $J/\psi \to 3\pi^o$ J/ψ, which produce significant numbers of low-energy photons. These may also be eliminated as sources because the resulting photon energy distributions are much too broad.

(iii) The possibility of some not-understood generally occurring effect in the detector is ruled out by the absence of similar structure in the J/ψ spectrum [Fig. 11(c)], where the statistics are comparable.

(iv) The possibility of a detector malfunction is ruled out by noting that the signal exists both in data taken in 1978-79 and in spring 1981 data, and by checking that the signal is not restricted to any particular region of the detector. [As a historical aside, the decision to double the data sample in spring 1981 was made for the purpose of checking the evidence in the earlier data. The fact that the effect repeated is a source of confidence.]

We conclude that the most likely explanation for the signal is that it is a new radiative decay of the ψ', presumably to the predicted 2^1S_0 $c\bar{c}$ state, the η_c'. Let us briefly compare its properties to the predicted η_c' properties, based on a potential model for charmonium. One quantity of interest is the relative size of the hyperfine splitting for

the radially excited state compared with the ground state:

$$R_{hfs}(2/1) = \frac{m(\psi') - m(\eta_c')}{m(J/\psi) - m(\eta_c)} . \qquad (7)$$

If we use the Crystal Ball values for these splittings (from the inclusive photon analysis), we find:

$$R_{hfs}(2/1) = 0.83 \pm 0.06 .$$

There are various statements in the theoretical literature concerning what this number should be (e.g., Refs. 22 and 23). A recent paper[22] suggests that a reliable estimate (at least with respect to perturbative corrections) is:

$$R_{hfs}(2/1) = \frac{|\psi_{2S}(0)|^2}{|\psi_{1S}(0)|^2} = \left[\frac{m(\psi')}{m(J/\psi)} \right]^2 \frac{\Gamma(\psi' \to e^+e^-)}{\Gamma(J/\psi \to e^+e^-)} \sec^2\theta \qquad (8)$$

where I have inserted the $\sec^2\theta$ factor in an attempt to see what effect the $2^3S_1 - 1^3D_1$ mixing might have[8] (θ is the mixing angle,[24] $\theta = 23 \pm 3^o$). Substituting in measured values for the parameters[18] yields:

$$R_{hfs}(2/1) = 0.73 \pm 0.12 .$$

The agreement between theory and experiment is reasonable (if we were to assume no 2S-1D mixing, we would predict $R_{hfs}(2/1) = 0.62 \pm 0.10$). The

predicted radiative rate for $\psi' \to \gamma\eta_c'$ is given by the same allowed M1 formula as for $J/\psi \to \gamma\eta_c$, Eq. (4), and with $E_\gamma = 91 \pm 5$ MeV, we expect: $BR(\psi' \to \gamma\eta_c') = (0.45 \pm 0.11)\%$, where the uncertainty is due to the uncertainty in E_γ, and the large uncertainty in $\Gamma_{tot}(\psi')$. This prediction is within the large range allowed by the observation. Likewise, the expected width for the state (~ few MeV), based simply on "gluon counting" arguments,[7] is also compatible with our limit.

The DESY-Heidelberg group reported evidence[25] for a state at a mass of 3591 ± 7 MeV in the exclusive channel $\psi' \to \gamma\gamma\ J/\psi \to \gamma\gamma\mu^+\mu^-$. In spite of the similarity in mass, a connection between their result and our observation appears very doubtful. First, we have looked with the Crystal Ball for evidence of such a state in $\psi' \to \gamma\gamma\ J/\psi \to \gamma\gamma\mu^+\mu^-$ or $\gamma\gamma e^+e^-$, with greater sensitivity than the DESY-Heidelberg experiment. No signal was found, and a 90% C.L. upper limit was set of[12] $BR(\psi' \to \gamma + 3591)\cdot BR(3591 \to \gamma\ J/\psi) < 0.04\%$, to be contrasted with their result of[25] $(0.18 \pm 0.06)\%$. Secondly, if we assume that the object we observe in the inclusive spectrum really is the η_c', then we can make an estimate for its radiative decay rate to the J/ψ. By noting that the $\eta_c' \to \gamma\ J/\psi$ decay should have the same hindered M1 matrix element, up to the difference in E_γ, as the $\psi' \to \gamma\eta_c$ transition, we can eliminate theoretical uncertainty due to the wave functions by using the measured $\psi' \to \gamma\eta_c$ rate and scaling appropriately:[7,26]

$$\frac{\Gamma(\eta_c' \to \gamma\ J/\psi)}{\Gamma(\psi' \to \gamma\eta_c)} = \left[\frac{E_\gamma(\eta_c' \to \gamma\ J/\psi)}{E_\gamma(\psi' \to \gamma\eta_c)}\right]^7 = 0.11 \pm 0.01\ . \quad (9)$$

Putting in the measured ψ' rate, this yields $\Gamma(\eta_c' \to \gamma\ J/\psi) =$ (69 ± 24) eV. The η_c' is expected to have a total width > 1 MeV (any substantially smaller width would be very surprising since the two gluon decay is allowed). Thus, we expect, with some confidence, that $BR(\eta_c' \to \gamma\ J/\psi) < 10^{-4}$. Combining this with our inclusive result, we expect $BR(\psi' \to \gamma\eta_c') \cdot BR(\eta_c' \to \gamma\ J/\psi) < 10^{-6}$, hence not observable in any existing analysis.

V. A LOOK AT THE J/ψ "ENDPOINT" PHOTON SPECTRUM

The radiative decays of the J/ψ to low-mass (relative to charmonium) states have long been of substantial interest. Recent excitment has centered around the possibility of observing a gluon-gluon resonance ("glueball") in these decays. The dominant decay of the J/ψ, in the perturbative gluon-counting picture, should be to 3 gluons, because decay to 1 or 2 gluons is forbidden (1 by color, 2 because a spin-1 particle cannot decay to two massless spin-1 particles[27]). Thus, the radiative decay where one of the gluons is replaced by a photon should occur with a branching fraction of order α/α_s:[7]

$$\frac{\Gamma(J/\psi \to \gamma gg)}{\Gamma(J/\psi \to ggg)} = \frac{36}{5}\left(\frac{2}{3}\right)^2 \frac{\alpha}{\alpha_s} . \qquad (10)$$

Experimentally, this is not an unreasonably small quantity, and if there exists one or more glueball states, one might hope to see evidence for them in the inclusive photon spectrum at the J/ψ.

Figure 13 shows the high energy end of the inclusive photon spectrum for J/ψ decays, as measured in the Crystal Ball. The prominent

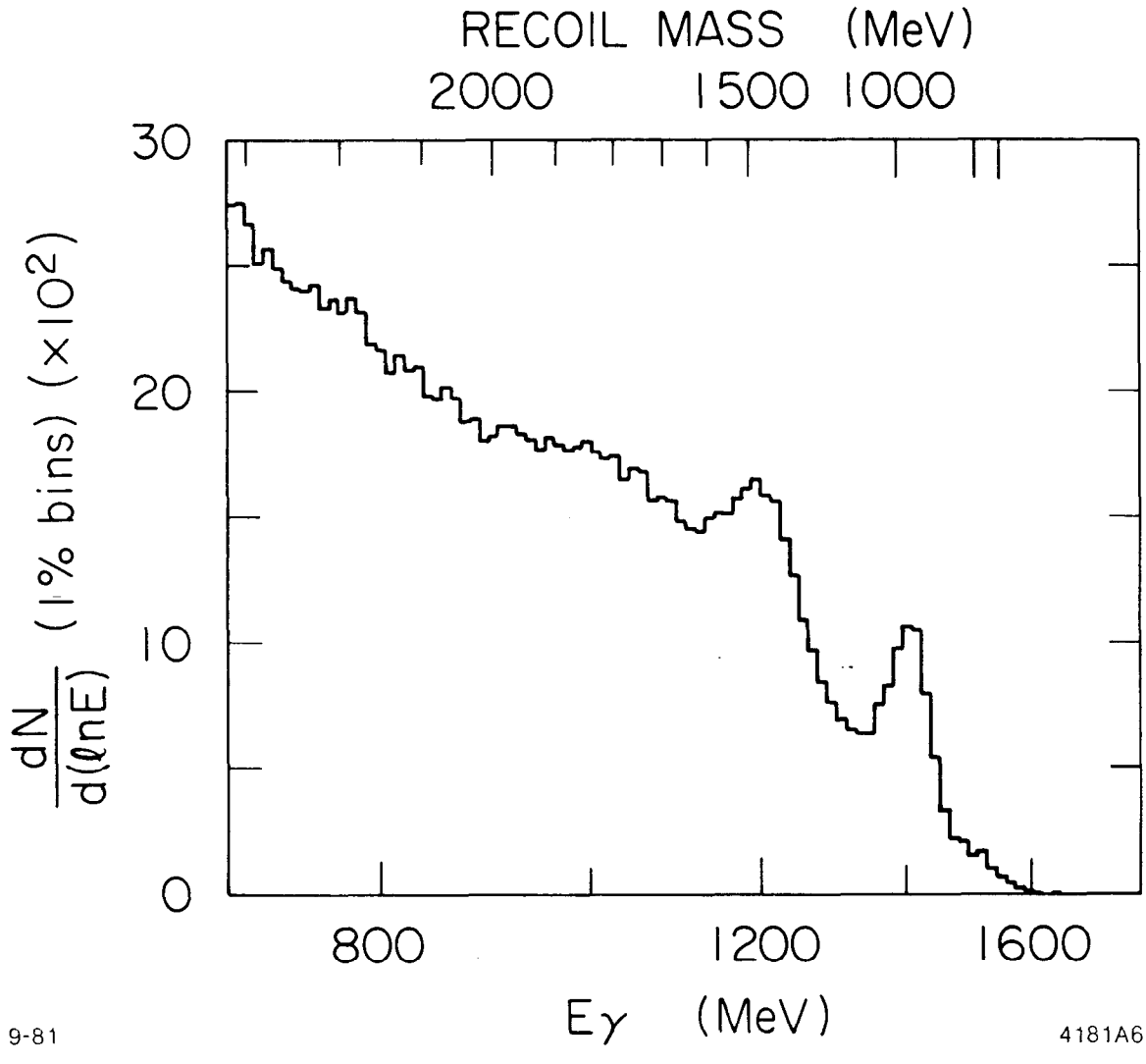

Fig. 13. The high energy end of the inclusive photon spectrum for J/ψ decays. The selection criteria are the same as for Fig. 8(e).

peak at $E_\gamma \sim 1400$ MeV is due to the $J/\psi \to \gamma\eta'$ decays. Transitions to the η would occur at $E_\gamma \sim 1500$ MeV, but are suppressed here because of the event selection cuts (especially, the QED and multiplicity cuts, see Sec. II-A). Likewise, even if the $J/\psi \to \gamma\pi^0$ branching ratio were large, no signal would be observed in this plot because of the event selection cuts. The selection efficiency tends to improve as the recoil mass increases, and, unless the state has very peculiar decays (e.g., to neutrinos), this efficiency is reasonable for m(recoil) $\gtrsim$ 1 GeV.

A second prominent peak occurs at $E_\gamma \sim 1200$ MeV. This corresponds most closely in recoil mass to the E-meson, among known particles, but there are arguments which suggest that it is not due to the E.[28] The tails of this peak include the regions where transitions to the f', f, and D mesons would appear. Below this second peak there is a broad bulge, extending down to $E_\gamma \sim 900$ MeV [or m(recoil) up to ~2000 MeV]. Whether this is caused by a series of closely space resonances, or perhaps a gluonic continuum, is not known.

So far, very little quantitative analysis of this spectrum has been done, so I have little more to say about it. One of the problems is that for $E_{\pi^0} \gtrsim 600$ MeV, the two gammas from many π^0 decays have sufficiently overlapping showers that the routine production analysis treats them as a single photon. The lateral shower pattern criteria suppress this background in Fig. 13, but there is probably still substantial contamination. Fortunately, more sophisticated algorithms for separating π^0 and single-γ showers have been developed recently, and the prospects for future analysis appear bright.

VI. SEARCH FOR HADRONIC $\chi \to J/\psi$ TRANSITIONS

The production of J/ψ mesons in hadronic interactions has been receiving substantial attention lately. The currently popular picture for hadronic J/ψ production is the "gluon fusion" idea, where two relatively hard gluons come together to form a $c\bar{c}$ pair.[29] Perturbation theory should be valid in this picture, so one must apply the appropriate "gluon counting" rules. Thus, the $c\bar{c}$ pair cannot directly be a J/ψ meson. One way to make the transformation to a J/ψ is by the emission of a soft gluon from one of the charmed-quark lines [Fig. 14(a)]. Another way is to first produce a χ meson, which then radiatively decays to a J/ψ [Fig. 14(b)]. Note that the χ particle in the gluon fusion diagram of Fig. 14(b) may be either the $\chi_2(3555)$ or $\chi_0(3410)$, but not the $\chi_1(3510)$. Also, since $BR(\chi_2 \to \gamma\ J/\psi) = (16 \pm 3)\%$ and $BR(\chi_0 \to \gamma\ J/\psi) = (0.61 \pm 0.16)\%$ (see Sec. II), the hadronic production of J/ψ via χ radiative decays will be dominated by the χ_2, unless for some reason the cross section for χ_0 production is much greater (by a factor $\gtrsim 25$) than that for χ_2 production [in the spirit of gluon counting, one might expect[7] $\sigma(\text{hadron} \to \chi_0 x)/\sigma(\text{hadron} \to \chi_2 x) \approx 15/4$]. Finally, let us note that the p-wave χ state of Fig. 14(b) could instead be the $^1S_0$, η_c'. However, as I pointed out in Sec. IV, the branching ratio for $\eta_c' \to \gamma\ J/\psi$ should be very small ($\lesssim 10^{-4}$), so the η_c' production cross section would have to be enormous for the process to compete with J/ψ production via $\chi_2 \to \gamma\ J/\psi$.

Motivated by an unexplained experimental result[30] in the hadronic production of J/ψ, the question has arisen whether the radiative transition in Fig. 14(b) might be replaced a significant fraction of the time

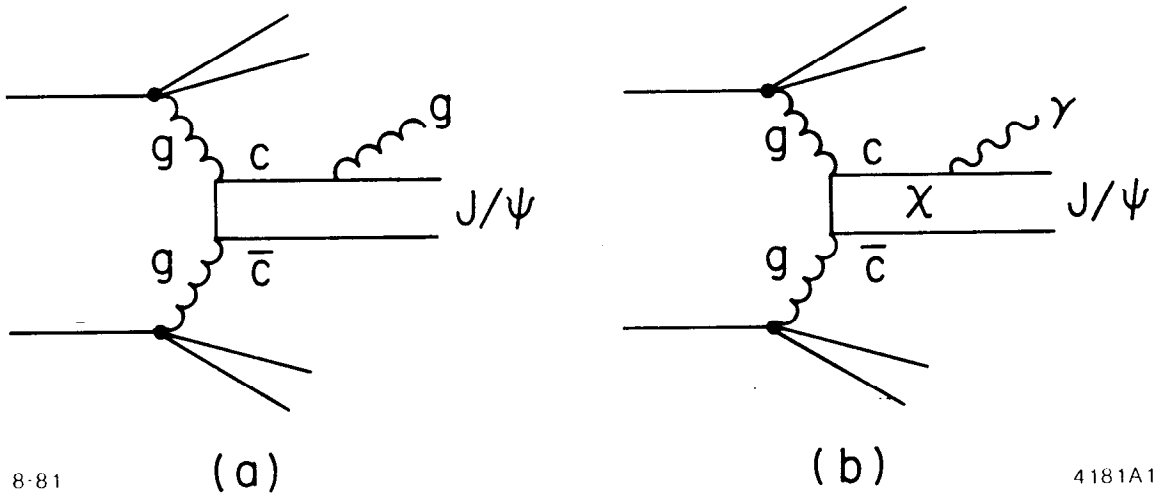

Fig. 14. Production of the J/ψ via gluon fusion in hadronic collisions: (a) Gluon fusion to $c\bar{c}$, becoming a J/ψ by emission of a soft gluon; and (b) gluon fusion to a χ state of charmonium, followed by a radiative decay to J/ψ.

by some hadronic decay -- are there any substantial $\chi \to J/\psi$ + hadrons channels? Most possibilities can be immediately ruled out by conservation laws, but two of those remaining have been given serious consideration, and we shall discuss them here.

A. Search for $\chi_2 \to \pi^+\pi^-\pi^o\ J/\psi$

The first to be suggested[31] was that the decay $\chi_2 \to \pi^+\pi^-\pi^o\ J/\psi$ might have a large branching fraction. This suggestion, however, disagrees with the prediction based on the multipole expansion technique.[32] We have searched for evidence of this decay in the Crystal Ball experiment by looking for the decay chain:

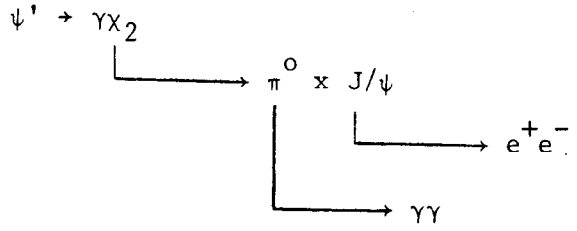

(11)

where "x" (in this case $\pi^+\pi^-$) is not required to be observed. The event selection is as follows:

(i) The number of observed charged particles must be in the range 2 to 5, and the number of observed neutrals must be in the range 3 to 5.

(ii) The event is required to have a $J/\psi \to e^+e^-$ decay by requiring the observed invariant mass of two charged particles to be between 2800 and 3200 MeV.

(iii) The event is required to have a $\pi^o \to \gamma\gamma$ decay by requiring at least one $\gamma\gamma$-mass combination in the range 115-155 MeV.

(iv) The event is required to have a slow π^o (as would occur from a $\chi_2 \to \pi^+\pi^-\pi^o$ J/ψ decay) by demanding that there be a π^o [as defined in (iii)] with energy less than 200 MeV.

The resulting inclusive photon spectrum for the remaining events is shown in Fig. 15(a). No evidence is seen for the monochromatic photon which would result from the decay $\psi' \to \gamma\chi_2$. After correcting for detection efficiency and the $\psi' \to \gamma\chi_2$ and J/$\psi \to e^+e^-$ branching ratios, we obtain the upper limit:

$$BR(\chi_2 \to \pi^+\pi^-\pi^o \text{ J/}\psi) < 0.05 \quad (90\% \text{ C.L.}) \ .$$

B. Search for $\chi \to \gamma\pi^o$ J/ψ

The second possibility to be suggested was that the $\chi \to$ J/ψ hadronic decay should be dominated by the ω-resonance amplitude, and that, because of the available phase space, the $\gamma\pi^o$ rate should be much larger than the $\pi^+\pi^-\pi^o$ rate.[33] The $\chi \to \gamma\pi^o$ J/ψ transition is allowed for all three χ states. We have searched for this process by looking at events fitting the exclusive hypothesis:

$$\psi' \to \gamma\gamma\pi^o \text{ J/}\psi \quad \begin{cases} \to e^+e^- \text{ or } \mu^+\mu^- \\ \to \gamma\gamma \ . \end{cases} \qquad (12)$$

Background from the $\psi' \to \pi^o\pi^o$ J/ψ decay is reduced by rejecting events which fit the $\pi^o\pi^o$ hypothesis with confidence level > 0.10. For each event with an acceptable fit to hypothesis (6-2), we take the fit with

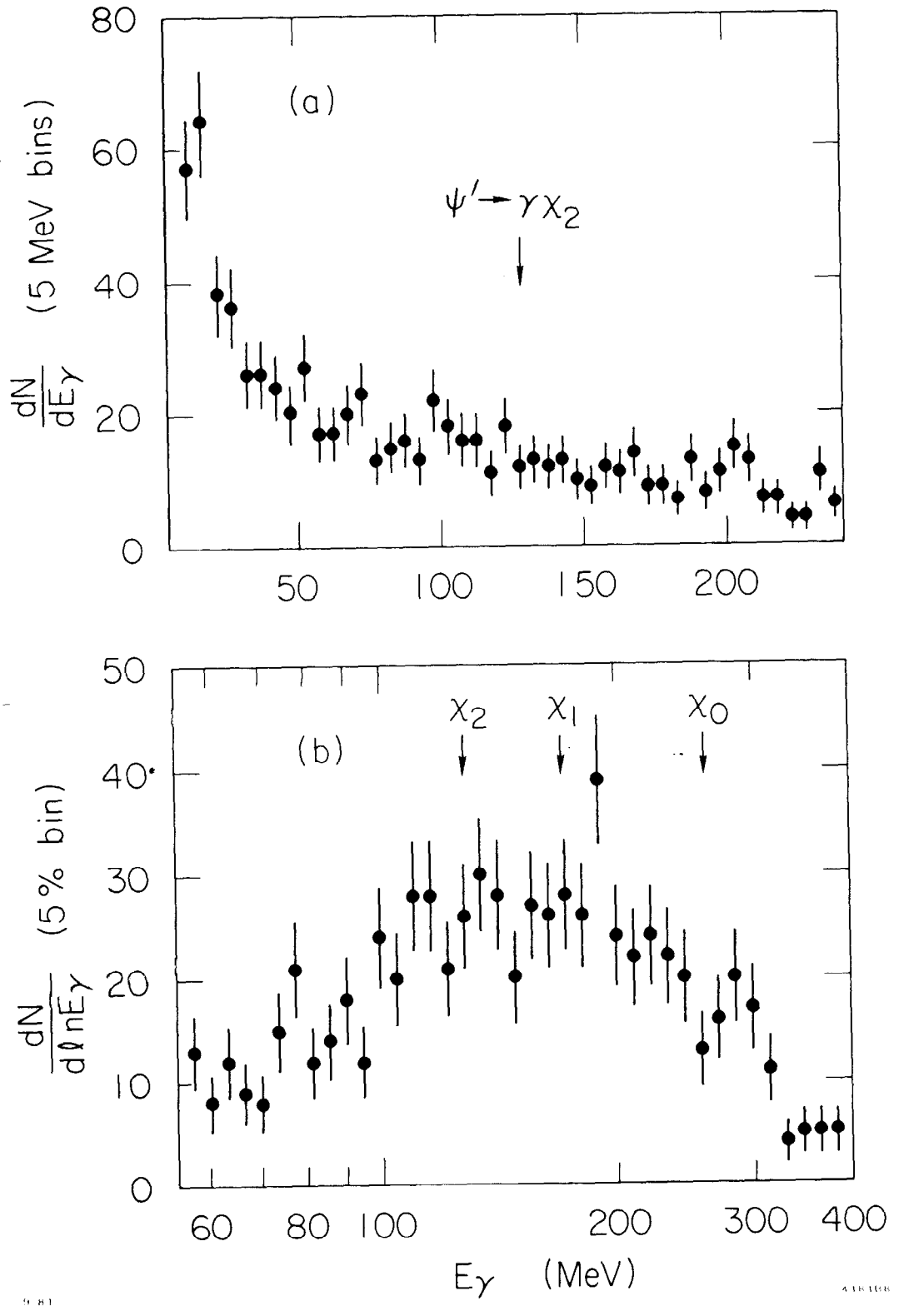

Fig. 15. (a) Search for $\chi_2 \to \pi^+\pi^-\pi^o$ J/ψ. The photon energy is plotted for ψ' decays which contain a slow π^o and a $J/\psi \to e^+e^-$ decay. (b) Search for $\chi_J \to \gamma\pi^o$ J/ψ. The photon energy is plotted for events which fit the hypothesis $\psi' \to \gamma\gamma\pi^o$ $J/\psi \to \gamma\gamma\pi^o\ell^+\ell^-$.

the best χ^2 and plot the photon energies (excluding the π^o decay photons) in Fig. 15(b). There is no convincing evidence for the monochromatic photons which would be expected from $\psi' \to \gamma\chi$ decays. Correcting for the detection efficiencies, and for the $\psi' \to \gamma\chi$ and $J/\psi \to \ell^+\ell^-$ branching fractions we obtain the following upper limits for $\chi \to \gamma\pi^o$ J/ψ:

TABLE III

Limits on $\chi \to \gamma\pi^o$ J/ψ

χ State	BR($\chi \to \gamma\pi^o$ J/ψ) (90% C.L.)
χ_0 (3410)	< 1.7%
χ_1 (3510)	< 3.0%
χ_2 (3555)	< 2.1%

To conclude this section, we have searched for the decays $\chi_2 \to \pi^+\pi^-\pi^o$ J/ψ and $\chi \to \gamma\pi^o$ J/ψ, and find no evidence for them. Our limits are sufficient to exclude these processes as the primary explanation for the peculiar effect observed in hadronic J/ψ production.

ACKNOWLEDGEMENTS

I would like to thank my colleagues on the Crystal Ball collaboration for many stimulating discussions. In particular, I am grateful to J. Gaiser and J. Tompkins for extensive discussions on the analysis of inclusive photon spectra.

REFERENCES

1. The Crystal Ball collaboration: California Institute of Technology, Physics Department - C. Edwards, G. Grey, C. Huscroft, R. Partridge, C. Peck, and F. Porter; Harvard University, Physics Department - D. Antreasyan, Gu Yifan, J. Irion, W. Kollmann, M. Richardson, K. Strauch, K. Wacker, and A. Weinstein; Princeton University, Physics Department - D. Aschman, T. Burnett, M. Cavalli-Sforza, D. Coyne, M. Joy, and H. Sadrozinski; Stanford Linear Accelerator Center - E. Bloom, F. Bulos, R. Chestnut, J. Gaiser, G. Godfrey, C. Kiesling, W. Lavender, J. Leffler, S. Lindgren, W. Lockman, S. Lowe, M. Oreglia, and D. Scharre; Stanford University, Physics Department and High Energy Physics Laboratory - D. Gelphman, R. Hofstadter, R. Horisberger, I. Kirkbride, H. Kolanoski, K. Königsmann, R. Lee, A. Liberman, J. O'Reilly, A. Osterheld, B. Pollock, and J. Tompkins.
2. D. L. Burke, SLAC-PUB-2745, to be published in the Proceedings of the 4th International Colloquium on Photon-Photon Interactions, Paris, April 6-9, 1981.
3. F. C. Porter, CALT-68-852, SLAC-PUB-2785, to be published in the Proceedings of the European Physical Society Conference on High Energy Physics, Lisbon, Portugal, July 9-15, 1981.
4. E. D. Bloom, to be published in the Proceedings of the XVIth Rencontre de Moriond, Les Arcs, France, March 15-27, 1981; W. S. Lockman, reported at APS meeting, Baltimore, April 20-23, 1981.

5. T. Appelquist, A. DeRújula, H. D. Politzer and S. Glashow, Phys. Rev. Lett. 34, 365 (1975); E. Eichten et al., Phys. Rev. Lett. 34, 369 (1975).

6. C. J. Biddick et al., Phys. Rev. Lett. 38, 1324 (1977).

7. For a review of charmonium, see: T. Appelquist, R. M. Barnett and K. Lane, Ann. Rev. Nucl. Part. Sci. 28, 387 (1978), J. D. Jackson, H. E. Gove and R. F. Schwitters, eds.

8. E. Eichten et al., Phys. Rev. D21, 203 (1980).

9. T. M. Himel et al., Phys. Rev. Lett. 45, 1146 (1980).

10. R. Partridge et al., Phys. Rev. Lett. 45, 1150 (1980).

11. T. M. Himel et al. Phys. Rev. Lett. 44, 920 (1980); M. Oreglia et al., Phys. Rev. Lett. 45, 959 (1980).

12. M. Oreglia, Ph.D. thesis, Stanford University, SLAC-236 (1980).

13. The material in this section comes primarily from the thesis research of J. Gaiser.

14. The "primary" event triggers are an "or" of a total energy requirement (typically, the energy in the central 90% of the solid angle is required to be $> \sim 1100$ MeV), or a multiplicity requirement (roughly, at least two tracks depositing $\gtrsim$ 120 MeV each in the NaI with at least one charged particle, or at least four tracks with $\gtrsim$ 120 MeV deposited by each).

15. R. L. Ford and W. R. Nelson, SLAC-210 (1978).

16. J. Arafune and M. Fukugita, KEK-TH22, contributed to the European Physical Society Conference on High Eneryg Physics, Lisbon, Portugal, July 9-15, 1981.

17. R. Barbieri, R. Gatto and E. Remiddi, Phys. Lett. 61B, 465 (1976); R. Barbieri, M. Caffo and E. Remiddi, Phys. Lett. 83B, 345 (1979); R. Barbieri, M. Caffo, R. Gatto and E. Remiddi, Phys. Lett. 95B, 93 (1980), and Ref.TH.3071-CERN, April 1981.

18. Except as noted, I use $m(J/\psi) = 3095$ and $m(\psi') = 3684$ MeV. Values for the following widths are taken from the Particle Data Group compilation [N. Barash-Schmidt et al., Rev. Mod. Phys. 52, No. 2 (1980)]: $\Gamma_{tot}(J/\psi) = 63 \pm 9$ keV, $\Gamma_{tot}(\psi') = 215 \pm 40$ MeV, $\Gamma(J/\psi \to e^+e^-) = 4.70 \pm 0.50$ keV, $\Gamma(\psi' \to e^+e^-) = 2.05 \pm 0.23$ [I assume that $\Gamma(n^3S_1 \to e^+e^-) = \Gamma(n^3S_1 \to \mu^+\mu^-)$].

19. R. Barbieri, G. Curci, E. d'Emilio and E. Remiddi, Nucl. Phys. B154, 53 (1979).

20. R. Partridge et al., Phys. Rev. Lett. 44, 712 (1980).

21. Beyond these, no other statistically significant narrow structure is found in the spectrum for $25 < E_\gamma < 1000$ MeV. In the region of the χ lines, of course, substantial signals could exist which we cannot separate from the χ lines. No detailed study has yet been made of the high end of the spectrum ($E_\gamma > 1000$ MeV), where structure is expected due to the presence of $\psi' \to \pi\pi$ J/ψ decays and the pronounced structure in the high energy end of the J/ψ decay spectrum (see Sec. V).

22. E. Eichten and F. Feinberg, Phys. Rev. D23, 2724 (1981).

23. A. Martin, Phys. Lett. 93B, 338 (1980); D. Beavis, Shu-Yuan Chu, B. Desai and P. Kaus, Phys. Rev. D20, 743 (1979); C. Quigg, in Proceedings of the 1979 International Symposium on Lepton and Photon Interactions at High Energies, ed. by T. Kirk and H. Abarbanel (1979), p. 239.

24. P. A. Rapidis et al., Phys. Rev. Lett. 39, 526 (1977).

25. W. Bartel et al., Phys. Lett. 79B, 492 (1978).

26. It is possible that relativistic effects alter the scaling expected in Eq. (9) [J. D. Jackson, in Proceedings of Summer Institute on Particle Physics, SLAC, 2-13 August 1976, Ed., M. C. Zipf, SLAC-198, pp. 147-202; G. Feinberg and J. Sucher, Phys. Rev. Lett. 35, 1740 (1975)]. However, even if we were to neglect scaling with the photon energy, the same conclusion would result.

27. C. N. Yang, Phys. Rev. 77, 242 (1950).

28. J. Donoghue, K. Johnson and Bing An Li, Phys. Lett. 99B, 416 (1981); M. Chanowitz, Phys. Rev. Lett. 46, 981 (1981).

29. C. Carlson and R. Suaya, Phys. Rev. D15, 1416 (1977); H. Fritzsch, Phys. Lett. 67B, 217 (1977); M. Glück, J. Owens, and E. Reya, Phys. Rev. D17, 2324 (1978); M. Glück and E. Reya, Phys. Lett. 79B, 453 (1978); Y. Afek, C. Leroy and B. Margolis, Phys. Rev. D22, 86 (1980).

30. T. Kirk, this institute; S. Pordes, reported at APS meeting, Baltimore, April 20-23, 1981.

31. R. Raja, FERMILAB-PUB-81/32-EXP, 1981 (submitted to Phys. Rev.).

32. C. Flory and I. Hinchliffe, LBL-12703, May 1981.

33. E. L. Berger and C. Sorensen, ANL-HEP-PR-81-28, July 1981.

34. After this was written, I received a preprint (R. McClary and N. Byers, UCLA/81/TEP/21, contributed to the International Symposium on Lepton and Photon Interactions at High Energies, Bonn, August 24-29, 1981) in which it is found that relativistic corrections to the E1 rates are substantial. Using a linear confinement plus modified one-gluon exchange potential, they find E1 rates which imply the following branching ratios:[18] $BR(\psi' \to \gamma\chi_J) = 0.088 \pm 0.016, 0.130 \pm 0.024, 0.126 \pm 0.023$ for $J = 0,1,2$, respectively. The rate for the χ_0 changes drastically with these corrections, and now agrees with observation. The rates for the $\chi_J \to \gamma\ J/\psi$ decays are found to be: $\Gamma(\chi_J \to \gamma\ J/\psi) =$ 111, 244, 310 keV for $J = 0,1,2$, respectively. The relativistic corrections have much less effect on these numbers, which are compatible within errors with current observation (Table II) whether the corrections are made or not.